Contribution of BKCa channels to vascular tone regulation by PDE3 and PDE4 is lost in heart failure

Sarah Idres, Germain Perrin, Valérie Domergue, Florence Lefebvre, Susana Gomez, Audrey Varin, Rodolphe Fischmeister, Véronique Leblais, Boris Manoury

Contribution of BK_{Ca} channels to vascular tone regulation by PDE3 and PDE4 is lost in heart failure

Sarah Idres[1], Germain Perrin[1], Valérie Domergue[2], Florence Lefebvre[1], Susana Gomez[1], Audrey Varin[1], Rodolphe Fischmeister[1], Véronique Leblais[1] and Boris Manoury[1].

[1] Signalling and cardiovascular pathophysiology - UMR-S 1180, Univ. Paris-Sud, INSERM, Université Paris-Saclay, 92296, Châtenay-Malabry, France

[2] UMS IPSIT, Univ. Paris-Sud, Université Paris-Saclay, 92296, Châtenay-Malabry, France

Short title: BK_{Ca}-mediated PDE regulation of artery tone

Correspondence to: B Manoury, UMR-S 1180, Faculté de Pharmacie, Université Paris-Sud, 5 rue J-B Clément, 92296 Châtenay-Malabry, France.

E-mail: boris.manoury@u-psud.fr; Tel: +33-1.46.83.59.06; Fax: +33-1.46.83.54.75.

Keywords: BK_{Ca} channel, phosphodiesterase, cAMP, coronary artery, heart failure

Word count: 8228

Total number of figures and tables: 8 main Figures, 4 supplementary Tables and 3 supplementary Figures.

Abstract

Aims

Regulation of vascular tone by 3',5'-cyclic adenosine monophosphate (cAMP) involves many effectors, including the large conductance, Ca^{2+}-activated, K^+ (BK_{Ca}) channels. In arteries, cAMP is mainly hydrolyzed by type 3 and 4 phosphodiesterases (PDE3, PDE4). Here, we examined the specific contribution of BK_{Ca} channels to tone regulation by these PDEs in rat coronary arteries, and how this is altered in heart failure.

Methods and Results

Concomitant application of PDE3 (cilostamide) and PDE4 (Ro-20-1724) inhibitors increased BK_{Ca} unitary channel activity in isolated myocytes from rat coronary arteries. Myography was conducted in isolated, U46619-contracted coronary arteries. Cilostamide or Ro-20-1724 induced a vasorelaxation that was greatly reduced by iberiotoxin, a BK_{Ca} channel blocker. Ro-20-1724 and cilostamide potentiated the relaxation induced by the β-adrenergic agonist isoprenaline or the adenylyl cyclase activator L-858051. Iberiotoxin abolished the effect of PDE inhibitors on isoprenaline but did not on L-858051. In coronary arteries from rats with heart failure induced by aortic stenosis, contractility and response to acetylcholine were dramatically reduced compared to arteries from sham rats, but relaxation to PDE inhibitors was retained. Interestingly, however, iberiotoxin had no effect on Ro-20-1724- and cilostamide-induced vasorelaxations in heart failure. Expression of the BK_{Ca} channel α-subunit and of a 98 kDa PDE3A was lower in heart failure compared to sham coronary arteries while that of a 70 kDa PDE4B was increased. Proximity ligation assays demonstrated that PDE3 and PDE4 were localized in the vicinity of the channel.

Conclusion

BK_{Ca} channels mediate the relaxation of coronary artery induced by PDE3 and PDE4 inhibition. This is achieved by co-localization of both PDEs with BK_{Ca} channels, enabling tight control of cAMP available for channel opening. Contribution of the channel is prominent at rest and on β-adrenergic stimulation. This coupling is lost in heart failure.

Abbreviations

AC: Adenylyl cyclase

ACh: Acetylcholine

α-s.u.: α-(pore forming) subunit of the BK_{Ca} channel

β-AR: Beta-adrenergic receptor

BK_{Ca}: Large conductance, Ca^{2+}-activated K^+ channel

CA: Coronary artery

cAMP: 3', 5'-cyclic adenosine monophosphate

cGMP: 3', 5'-cyclic guanosine monophosphate

Cil: Cilostamide

CRC: Concentration-response curve

IBTX: Iberiotoxin

ISO: Isoprenaline

HF: Heart failure

K_V: Voltage-dependent K^+ channel

K_{ATP}: ATP-sensitive K^+ channel

K80: 80 mmol/L KCl -modified Krebs solution

LADCA: Left anterior descending coronary artery

LV: Left ventricle

NP_o: Average number of open channels

NF_o: Opening frequency of N channels

PDE: Cyclic nucleotide phosphodiesterase

PLA: Proximity ligation assay

PP: Patch potential

Ro: Ro-20-1724

RyR: Ryanodine receptor

VSMC: Vascular smooth muscle cell

1. Introduction

Adequate vasoreactivity of the coronary circulation is key for cardiovascular homeostasis. However coronary reserve is altered in cardiac hypertrophy and heart failure (HF)[1-5]. Abnormal coronary flow in HF may originate from arterial wall remodelling, atherothrombosis and vascular rarefaction. In addition, endothelial-dependent vasodilatation and relaxant responses initiated by 3',5'-cyclic adenosine monophosphate (cAMP)-elevating agents[6-8], have been reported in patients with chronic HF[1, 6] and animal models of HF[7-9].

Production of cAMP is achieved by adenylyl cyclase (AC), while its hydrolysis is catalyzed by cyclic nucleotide phosphodiesterases (PDEs). There are 11 described families of PDEs that encompass 21 genes and a myriad of variants[10]. PDE3 and PDE4 are classically reported to account for the major part of the Ca^{2+}-independent, cAMP-PDE activity in vascular smooth muscle cells (VSMCs) from various species[11, 12]. Selective pharmacological inhibition of PDE3 or PDE4 is well known to elevate cAMP concentration in tissue[12, 13] and to promote relaxation of VSMCs in various vascular beds, including coronary artery (CA)[13-15]. This response is generally considered to be mediated by protein kinase A[16], although cross-activation of protein kinase G[17] and stimulation of exchange protein directly activated by cAMP (EPAC)[18, 19] are also documented. The potential downstream mechanisms that can be targeted by these pathways are numerous, encompassing effectors of Ca^{2+} handling and regulators of the Ca^{2+} sensitivity of the contractile apparatus[16].

Nevertheless, it remains unclear whether PDE3 and PDE4 control evenly cAMP concentrations in all compartments of VSMCs, or rather work by restricting cAMP in the vicinity of some particular effectors that would be predominant for the relaxing effect evoked by PDE inhibition. Importantly, evidence gathered by our laboratory and others in various models suggest that specific PDE subfamilies are non-uniformly localized near discrete cellular effectors and thus delineate restricted compartments that hinder the spreading of cAMP[10, 20]. According to this paradigm, such a compartmentalization would allow fine tuning of cAMP signals, and disorganization of these signalling platforms in disease might jeopardize cellular homeostasis[20]. In blood vessels, the actual existence of tone–regulating signalling domains that would include PDE3 and PDE4 remains elusive. Although already examined in endothelial cells[10], the potential tethering of PDE with molecular effectors of the cAMP pathway has never been investigated in contractile vascular smooth muscle layer.

Large conductance, Ca^{2+}-activated K^+ (BK_{Ca}) channels are key regulators of vascular and non-vascular smooth muscle tone[21-23]. Activation of BK_{Ca} channels by intracellular Ca^{2+} influx or local and transient Ca^{2+} release from the ryanodine receptor (i.e. Ca^{2+} sparks)[23, 24] repolarizes membrane potential, limiting Ca^{2+} influx through voltage-gated channels and hence contraction

of the VSMCs. In addition, BK_{Ca} channels are well documented cellular effectors of cAMP signalling in VSMCs: i) pharmacological inhibition of BK_{Ca} channels reduces the relaxing effect of cAMP-elevating agents [25, 26]; ii) the BK_{Ca} current is enhanced by such agents, an effect that may either be promoted directly by phosphorylation[21], or indirectly *via* potentiation of Ca^{2+} sparks[26, 27]. Of note, BK_{Ca} channel activity was reported to be depressed in several animal models of cardiovascular disorders[22] including HF[28].

Because the BK_{Ca} channel is a target of the cAMP pathway with pivotal role in regulation of vasomotricity, we tested the hypothesis that BK_{Ca} channels may be key effectors by which PDE3 and PDE4 control vascular tone in rat CA. We explored the modalities of such a coupling, and how this is impacted by the establishment of HF.

2. Materials and Methods

An expanded detailed version of Materials and Methods is available online.

2.1 Animals and surgical procedures

All animal care and experimental procedures conformed to the European Community guiding principles in the care and use of animals (2010/63/EU) and complied with French institution's application decrees for animal care and handling. Aortic stenosis was mimicked in rats under anaesthesia and analgesia, by placing a stainless steel hemoclip (0.6 mm-internal diameter) on the ascending aorta via thoracic incision, as previously described[29]. The surgical procedure was carried out on 3-week-old rats, under anaesthesia with a ketamine-xylazine mix (75 mg/kg – 10 mg/kg, respectively, 0.3 mL/100g, i.p.). Buprenorphine chlorhydrate (0.2 mL/100g, s.c.) was administered twice daily for 3 days beginning at the end of the surgery. Age-matched sham animals underwent the same procedure without placement of the clip. Operated animals were sacrificed 22 weeks after surgery, using sodium pentobarbital (150 mg/kg, i.p).

2.2 Coronary artery isolation and smooth muscle cells preparation

Male, 8-10-week-old Wistar rats or above-mentioned operated rats were anesthetized by injection of pentobarbital (150 mg/kg, i.p). The left anterior descending coronary artery (LADCA, inner diameter 100–300 µm) was carefully isolated and either freshly used for vascular reactivity, submitted to digestion steps in order to obtain isolated smooth muscle cells (SMCs) used for patch-clamp or *in situ* immunolabelling, or immediately frozen for biochemical analysis.

2.3 cAMP-PDE activity assay and PDE inhibitors

cAMP-PDE activity was measured by a radioenzymatic assay according to the method reported by Thompson and Appleman[30] and adapted to vascular tissue[31]. Reactions were carried out with or without PDE inhibitors, namely 100 µmol/L IBMX, as a non-selective PDE inhibitor, 1 µmol/L cilostamide (Cil.), as a selective PDE3 inhibitor and 10 µmol/L Ro-20-1724 (Ro), as a selective PDE4 inhibitor (Table S1). IBMX-sensitive PDE activity, PDE3 and PDE4 activities were defined as the fraction of total activity that was inhibited by corresponding inhibitor.

2.4 Vascular reactivity measurement

Assessment of vascular reactivity was conducted in segments of LADCA mounted on wire myograph (DMT, Aarhus, Denmark), as previously described[32]. Vessels were isolated and mounted in "Krebs" solution (in mmol/L): NaCl 119, KCl 4.7, $CaCl_2(H_2O)_2$ 2.5, $MgSO_4(H_2O)_7$ 1.2, KH_2PO_4 1.2, glucose 11, $NaHCO_3$ 25, bubbled with 95% O_2 and 5% CO_2. All vessels were transiently challenged with 80 mmol/L KCl -modified Krebs solution (K80) to evaluate contractile capacity. Endothelial function was evaluated in all vessels by measuring the relaxation induced by 1 µmol/L acetylcholine (ACh) following contraction with the thromboxane A_2 mimetic U46619 (0.3-3 µmol/L) so as to obtain a response as close as possible to the ΔK80 response. In experiments set out to study the vasorelaxant effect of PDE inhibition, the rings were contracted with U46619 (0.3-3 µmol/L). Once steady contraction was obtained, Cil was added. To study the additional effect of PDE4 inhibition, PDE4 inhibitor Ro (10 µmol/L) was added on top of Cil. In other vessels, this order was reversed. In other experiments, vasorelaxant agonists were added on U46619-contracted vessels in a stepwise, cumulative fashion to establish concentration-response curve (CRC). When addressing the role of ion channels or PDEs in relaxant responses, inhibitors or relevant vehicle were applied during 10 min before U46619. Contractile responses were expressed in mN/mm and relaxant responses were expressed in %, relative to the contraction amplitude obtained with U46619.

2.5 Patch-clamp experiments

Unitary channel activity recording was performed in freshly isolated LADCA SMCs, using either cell-attached or inside-out configurations of the patch-clamp technique[17, 33]. Composition of extracellular bath solution was[34] (mmol/L): KCl 140, $MgCl_2$ 10, $CaCl_2$ 0.1, Hepes 10, D-glucose 30, pH=7.2 adjusted with KOH. High K^+ concentration in the bath was used to clamp cell membrane potential close to 0 mV. Experiments were conducted at room temperature (20-23°C). For cell-attached recordings, pipette (2-5 MOhm) solution[34] contained (mmol/L): KCl 5, NaCl 110, $MgCl_2$ 1, $CaCl_2$ 2, Hepes 10, pH=7.4 adjusted with NaOH. In some experiments, 0.1 µmol/L iberiotoxin (IBTX) was added in the pipette solution. Current was recorded at a patch

potential (PP) of 40 mV. Perfusion with PDE inhibitors was started after the vehicle (DMSO 0.03%) had been perfused for 2-5 min and channel activity was stable. Channel activity was analyzed using PClamp 10 (Molecular Devices Inc., Sunnyvale, CA, USA) and average number of open channels (NP_o), mean open time, opening frequency (NF_o) and unitary current amplitude were calculated. For inside-out recordings, pipette contained (mmol/L): KCl 140, $MgCl_2$ 1, $CaCl_2$ 0.1, Hepes 10, pH=7.4 adjusted with KOH. Several PP were tested to build up the current-PP relationship of the conductance detected.

2.6 Western Blot analysis

Western blotting was performed as previously described using other vascular tissues[31]. Protein samples were prepared in standard loading buffer under reducing conditions and heated at 95°C for 5 min except for BK_{Ca} detection. Following primary antibodies were used: rabbit anti-PDE3A (1/10000; kind gift from Dr. Chen Yan, University of Rochester Medical Center, NY, USA), anti-PDE4A (1/5000); rabbit anti-PDE4B (1/1000), anti-PDE4D (1/1000), kind gifts from Dr. Marco Conti (University of California, San Francisco, CA, USA); and a mouse anti-BK_{Ca} α-subunit (α-s.u. 1/500; #75-022, purchased from University of California Davis/NIH). GAPDH was used for normalization. Results were expressed relatively to the mean expression level in the sham group.

2.7 Proximity ligation assay (PLA)

PLA protocol was carried out according to the recommendation of manufacturer (Duolink® PLA, Sigma-Aldrich, St Quentin-Fallavier, France) using fixed LADCA SMCs. The following primary antibodies were used at the indicated dilutions: above-mentioned anti-BK_{Ca} α-s.u. (1/300), anti-PDE3A (1/400), anti-PDE4B (1/100), or a pan-PDE4 (rabbit, 1/100; #PD4-101AP, FabGennix, Frisco, TX, USA). Preparations were incubated overnight at 4°C with the anti-BK_{Ca} α-s.u. antibody and one type of anti-PDE antibody. Preparations incubated with only one antibody were used as negative control. Subsequent steps and image acquisition were performed using similar parameters for all slides testing a given antibody association. PLA images were acquired with a laser scanning confocal microscope (excitation: 554 nm; emission: 579 nm). Using the ImageJ 1.50b software all single cell images corresponding to one given couple of antibodies were converted into 8-bit and binarized using a common threshold value. Results were expressed as the percentage of cell area covered by PLA signal. Considering the average diameter of an antibody being 10 nm, this technique allows to detect co-localization of proteins in a 40 nm range.

2.8 Histological evaluation of coronary arteries

Following sacrifice, some hearts were prepared for paraffin inclusion. Sections (5 µm-thick) were stained by the trichrome method and digitally scanned. Wall thickness over vessel diameter ratio was analyzed using the ImageJ software.

2.9 Data and statistical analysis

CRCs obtained for each vessel were fitted with the Hill equation using Prism 7 software (Graphpad Software, La Jolla, CA, USA) and pharmacological parameters, namely pD_2 and maximal effect (E_{max}), were obtained. Data were expressed as mean ± SEM. N represented the number of rats while n represented the number of cells in electrophysiology and PLA experiments. Two-group comparisons were performed using either t-test, Welsh's t-test, or non-parametric Mann-Whitney test when relevant, except for paired comparisons that were performed using the Wilcoxon signed-rank paired test. In comparisons involving more than 2 groups, 1-way ANOVA followed by Holm-Sidak multiple comparison post-test was used. When comparing the effect of IBTX in sham and HF animals, 2-way ANOVA was used. Comparison of CRCs was performed using 2-way ANOVA for repeated measures. Where relevant, a nested ANOVA was performed to fit a mixed effect model. Values of $P<0.05$ were considered for statistical significance.

3. Results

3.1 Characterization of PDE3 and PDE4 activity in rat coronary artery

Because previous studies[12, 31] demonstrated that PDE3 and PDE4 were the most abundant cAMP-PDEs in vasculature, we first verified their respective contributions in rat LADCA. Total cAMP-hydrolyzing activity amounted to 76±11 pmol/min/mg (N=7 with tissue collected from 23 rats). Selective PDE3 inhibitor, Cil, (1 µmol/L), and selective PDE4 inhibitor, Ro (10 µmol/L), inhibited 55±5% and 33±2% of the total PDE activity, respectively (N=5-6). In comparison, the non-selective PDE inhibitor, IBMX (100 µmol/L) decreased the total PDE activity by 91±3% (N=4). These results confirm that PDE3 and PDE4 are the main contributors to cAMP hydrolysis in rat LADCA.

3.2 BK_{Ca} channels largely contribute to vasorelaxation induced by PDE3 and PDE4 inhibition

To address whether vasoactive effects of PDE3 and PDE4 inhibition are mediated by BK_{Ca} channels, we applied Ro or Cil on rat LADCA mounted on a wire-myograph and contracted with U46619 (0.3-3 µmol/L, Table S2A), in the presence or absence of IBTX (0.1 µmol/L), a

selective BK_{Ca} channel inhibitor (Table S1). Figure 1A-B shows that Cil and Ro relaxed contracted LADCA on average by 40±11% and 26±5%, respectively. Both Ro and Cil effects were greatly blunted by IBTX. Furthermore, joint addition of Cil and Ro induced a synergistic relaxation which was still significantly decreased by ≈50% upon IBTX pretreatment. These results provided evidence that, in rat LADCA, the vasorelaxant effect of PDE3 or PDE4 inhibitors involves activation of BK_{Ca} channels. IBTX was still as effective in inhibiting relaxant response to combined Ro and Cil in LADCA rings where the endothelium had been voluntarily deteriorated (Figure 1C), showing that the coupling between PDE3/4 and BK_{Ca} channel takes place in the smooth muscle layer and is not influenced by endothelium-derived components. The contributions of alternative vascular K^+ channels were also investigated in precontrated LADCA (Table S2A) using selective inhibitors (Table S1). Interestingly the K_v7 blocker XE991 (30 µmol/L) also inhibited the action of combined Ro and Cil, while DPO-1 (1 µmol/L), stromatoxin-1 (0.1 µmol/L), selective blockers of K_v1 and K_v2 channels, respectively, or the K_{ATP} channel blocker glibenclamide (10 µmol/L) had no effect (Figure 1D). These data indicate that the relaxing effects of Ro and Cil in rat LDCA require specific activity of BK_{Ca} and K_v7 channels.

Ca^{2+} sparks can activate BK_{Ca} channels and regulate smooth muscle tone[24]. Thus, to address the relevance of this pathway in the relaxant effect of PDE3/4 inhibition in precontracted rat LADCA, we repeated the above protocol using high concentration of ryanodine (30 µmol/L, Table S1-S2A) to prevent Ca^{2+} release from internal stores via the ryanodine receptor (RyR). We found that, in contrast to IBTX, ryanodine did not significantly alter the relaxant responses induced by Cil and Ro. This indicates that ryanodine-sensitive BK_{Ca} channel regulation is not a prominent mechanism in the relaxation induced by PDE3/4 inhibitors in rat LADCA.

3.3 Simultaneous inhibition of PDE3 and PDE4 increased BK_{Ca} channel activity

In order to verify whether PDE3 and PDE4 control the activity of BK_{Ca} channels, we examined the effect of inhibition of PDE3 or PDE4 on BK_{Ca} channel activity in freshly isolated LADCA SMCs. Using inside-out patches in symmetrical $[K^+]$ and bath with high $[Ca^{2+}]$ (0.1 mmol/L), a unitary conductance of 221 pS was measured, consistent with properties of BK_{Ca} channel in VSMCs (Figure S1A). Using the cell-attached configuration of the patch-clamp technique and physiological K^+ gradient, channel activity was observed in most membrane patches and was dramatically silenced when pipette solution contained IBTX (Figure S1B), strongly supporting that this conductance was carried by BK_{Ca} channels. Average unitary current in the presence of 0.03% DMSO amounted to 5.4±0.4 pA, at a 40 mV PP, and the channel open state probability NP_o averaged to 0.029±0.006 (n=26), consistent with other reports in similar conditions[17]. Figure 2 and Table S3 show the effects of PDE3 and PDE4 inhibition on channel

activity in cell-attached patches. When perfused alone, Ro or Cil had no obvious effect on channel activity. However, simultaneous perfusion with Ro and Cil significantly increased NP_o, mean open time and NF_o. Thus BK_{Ca} channel activity can be regulated by PDE3 and PDE4.

3.4 BK_{Ca} channels participate in the potentiating effect of PDE3 and PDE4 inhibitors on the vasorelaxation induced by β-adrenergic or AC stimulation

So far, we have shown that BK_{Ca} channels are key players in the relaxing effect of PDE inhibitors on rat LADCA rings under resting cAMP level. In order to investigate the relevance of this phenomenon under stimulation of the cAMP pathway, the response of LADCA to isoprenaline (ISO), a β-adrenergic receptor (β-AR) agonist, was examined (Figure 3A-D, Table S2B). ISO induced a concentration-dependent relaxation of LADCA rings (pD_2=7.7±0.1, E_{max}=90±4%, Figure 3A). Both PDE4 (Ro, 10 µmol/L) and PDE3 (Cil, 1 µmol/L) inhibition shifted the CRC of ISO to the left and increased its pD_2 value to 8.3±0.1 and 8.2±0.1, respectively (P<0.01 for both), indicating a potentiating effect (Figure 3A and C). Pretreatment with IBTX reduced the E_{max} of ISO response to 54±4% (P<0.001) but not its pD_2 (7.6±0.1; Figure 3B and D). Interestingly, neither Ro nor Cil had any effect on ISO response in the presence of IBTX (Figures 3B and D). These results indicate that BK_{Ca} channels are important effectors of the β-adrenergic vasorelaxation. They further highlight a key role of BK_{Ca} channels in mediating the potentiating effect of PDE4 inhibition and PDE3 inhibition on this β-adrenergic response.

We also studied the effects of PDE3 and PDE4 inhibition on the response to a direct AC activator, L-858051 (L-85, a hydrophilic forskolin analog, (Figure 3E-H, Table S2C). L-85 induced a concentration-dependent relaxation (pD_2=6.5±0.1) which was potentiated by Ro and Cil (pD_2=7.1±0.1, P<0.001, and 6.8±0.1, P<0.05, respectively; Figure 3E and G). IBTX hampered the response to L-85, by decreasing its pD_2 value to 5.9±0.1 (P<0.001; Figure 3F and H). Interestingly, Cil and Ro still potentiated L-85 response in the presence of IBTX (Figure 3F and H). These data indicate that the potentiating effect of PDE3/4 inhibitors on the vasorelaxant response to direct AC stimulation does not require functional BK_{Ca} channels.

3.5 The coupling of BK_{Ca} channels with PDE3 and PDE4 is functionally absent in HF LADCA

We then explored whether the above-described coupling between BK_{Ca} channels and PDE3/4 is altered in HF situation, by using a rat model of chronic cardiac pressure overload[31]. Echocardiographic analysis in independent series of animals are presented in Table S4. Rats which had aortic stenosis surgery displayed significant increases in left ventricle (LV) mass, end diastolic and end systolic volumes, and a significant decrease in LV ejection fraction (EF) compared to sham-operated animals. Thus this model is featured with hypertrophic

remodelling of the myocardium, LV dilation and decreased systolic function. The weight of the lung normalized to tibia length (LW/TL) collected after sacrifice in rats with aortic stenosis correlated significantly with the decrease in systolic function (*e.g.* EF, P<0.05, Pearson correlation coefficients), and with the increase in LV dimensions (*e.g.* end-diastolic and end-systolic volumes, P<0.05 and P<0.01, respectively) and parameters related to LV hypertrophy (*e.g.* LV mass, P<0.01). Heart weight correlated only with LV mass and posterior wall thickness, diastolic (P<0.01) and systolic (P<0.001). Because the outcome of the model showed great individual variability[29], only rats with LW/TL ratio on sacrifice above 650 mg/cm, (as an evidence of lung congestion, a sign of HF) were included in the series used for experiments on LADCA (Figure 4A). Furthermore, histological examination revealed that CA from HF animals displayed thickening of their wall and perivascular fibrosis (Figure 4B).

LADCA isolated from HF rats (HF-LADCA) showed decreased contractile capacity to both K80 and U46619 (1 µmol/L), compared to LADCA isolated from sham rats (Figure 4C and Table S2D). Moreover, HF-LADCA displayed a significant reduction of the relaxant effect of ACh, an archetypical endothelium-mediated response, in comparison with sham (Figure 4D). Thus HF-LADCA are characterized by an alteration of their contractile capacity, accompanied by signs of endothelial dysfunction.

As already shown above, Ro relaxed sham-LADCA and this effect was prevented by IBTX (Figure 5A). By contrast, the relaxant response to Ro was not affected by IBTX (Figure 5A). Cil effect was less robust in this series in sham, but was globally higher in HF (P<0.01, 2-way ANOVA), with no effect of IBTX. (Figure 5B). Furthermore, upon simultaneous application of Ro and Cil, synergistic relaxant responses were observed in both HF- and sham-LADCA but the response was depressed by IBTX in sham-LADCA only (Figure 5C). Therefore, contribution of BK_{Ca} channel to the relaxing effect of PDE3/4 inhibition is lost in HF-LADCA.

3.6 Expression level of BK_{Ca} α-subunit, PDE3 and PDE4 in HF-LADCA

In order to provide a molecular basis that would explain this last result, we characterized the expressions of BK_{Ca} channel and PDE3/4 in sham- and HF-LADCA (Figures 6 and S2). The amount of the pore-forming α-s.u. of the BK_{Ca} channel was about half-decreased in HF- compared to sham-LADCA (Figure 6A). Quantification of PDE3A revealed a 2-fold decrease in a short, ≈98 kDa isoform, whereas a robust 4-fold increase in the amount of a 70 kDa PDE4B isoform was found in HF- compared to sham-LADCA (Figure 6B). PDE4A and PDE4D did not reveal any significant difference between HF and sham.

3.7 Proximity between PDE3/4 isoforms and BK_{Ca} channels

In order to reveal whether PDE isoforms localize in the vicinity of BK_{Ca} channels, experiments using PLA were performed in SMCs freshly isolated from either HF- or sham-LADCA. In sham-LADCA SMCs, PLA signals were detected using the antibody against the α-s.u. of the BK_{Ca} channel associated with either a PDE3A antibody, a pan-specific PDE4 antibody (documented to detect PDE4A and PDE4D isoforms) or a PDE4B antibody (Figure 7). Controls incubated with only one of these antibodies showed no signal except for the pan-specific PDE4 antibody (Figure S3). However, this signal was considered to be negligible compared to the signal obtained by coupling with anti-BK_{Ca} antibody. Quantification and mixed model analysis revealed no significant changes of the PLA signals in HF-LADCA cells.

4. Discussion

Here, we addressed the extent and modalities of the contribution of BK_{Ca} channels in mediating the vasodilating properties of PDE3 and PDE4 inhibitors. This was performed using rat LADCA isolated from either healthy rats or animals with severe HF. We report novel findings: (i) The existence of a signalosome involving PDE3/4 and BK_{Ca} channels is supported by PLA data that revealed *in situ* spatial proximity between PDE isoforms and the channel within a 40 nm range. (ii) PDE3 and PDE4 control BK_{Ca} channel activity. (iii) The relative contribution of BK_{Ca} channel to the relaxing effects of selective PDE inhibitors depends on the status of cAMP synthesis (either unstimulated, stimulated via β-AR, or direct AC stimulation) and is globally equivalent for PDE3 and PDE4. (iv) Inhibition of the RyR did not affect the relaxant responses to PDE3 or PDE4 inhibition. (v) In a model exhibiting signs of severe HF associated with hypertrophic remodelling of the myocardium, LV dilation and decreased systolic function, the contribution of BK_{Ca} channel to the regulation of coronary tone by PDE3 and PDE4 disappeared, although PDE3 and PDE4 inhibitors were still able to relax the vessels. This was associated with decreased expression of BK_{Ca} channel α-s.u. and of a short form of PDE3A. Altogether, these data provide new insights on how regulation of a specific cAMP effector by PDEs translates into fine-tuning of the vascular tone. Moreover, our study provides an unprecedented observation of an altered coupling between vascular PDEs and a cAMP effector, namely the BK_{Ca} channel, in a cardiovascular disorder.

4.1 Differential participation of BK_{Ca} channel to the relaxant action of PDE3/4 inhibition

Effects obtained with PDE3 and PDE4 inhibitors at selective concentrations (Table S1) were overall consistent with previous data obtained in various vascular beds[11-13, 15, 31, 35]. Using selective block with IBTX, we demonstrated that vasorelaxation by PDE3 or PDE4 inhibition in

rat LDCA depended substantially on BK_{Ca}. Few studies formerly explored such participation of BK_{Ca} channels in the relaxation evoked by PDE3/4 inhibition in other vascular beds. Regarding PDE3 inhibition, BK_{Ca} inhibitors showed either no or little effect in human or guinea-pig pulmonary artery (PA), respectively[36, 37]. In line with our study, Li et al.[38] reported that relaxation of rabbit aorta by cilostazol, a PDE3 inhibitor, was almost suppressed by the BK_{Ca} channel blocker paxilline. Considering PDE4 inhibition, a couple of reports mentioned that the relaxant effect of rolipram was only partially inhibited by BK_{Ca} inhibitors in human PA[36] and porcine CA[13]. Although heterogeneity of conclusions among reports may originate from diversity of protocols used (e.g. type and concentration of contractile agonist or PDE inhibitor used), the relative contribution of BK_{Ca} channels may also vary among vascular beds and species.

According to our data, K_v7 channels are interesting supplementary candidates for mediating the effects of PDE3 and PDE4 inhibitors. $K_v7.1$, $K_v7.4$ and $K_v7.5$ subunits were reported to be robustly expressed in rat CA[39] and inhibited by 30 µmol/L XE991 (Table S1). Accumulating evidence suggest that K_v7 act in parallel with BK_{Ca} channels to mediate cAMP vasorelaxant pathways in various vascular beds[19, 39]. Since PDE4 inhibition with rolipram was recently shown to enhance native $K_v7.5$ while $K_v7.4$ was insensitive[40], channels including the $K_v7.5$ subunit may contribute to the XE991-sensitive action of PDE inhibitors in our study.

We found that in rat LADCA SMCs, simultaneous PDE3 and PDE4 inhibition induced a clear stimulation of BK_{Ca} unitary channel activity. However, neither PDE3 nor PDE4 inhibitor used alone was sufficient to increase NP_o. Cilostazol was recently reported to stimulate channel activity in rabbit aortic SMCs[38]. However, a high concentration was used (10 µmol/L) so that the effect may also be attributed to other PDEs, such as PDE5[41]. Inhibition of a single PDE may not be sufficient for detectable increase of channel activity possibly because of overlapping activity of PDE3 and PDE4. Absence of endothelial-derived NO-cGMP pathway in isolated myocytes may enhance PDE3 activity and mask the effect of PDE4 inhibition[9, 11, 12]. Why then PDE3 inhibition had no apparent effect is unclear. At a low basal rate of cAMP production, inhibition of a single PDE family may only yield small or sporadic rise in cAMP concentration resulting in small increase in BK_{Ca} channel activity. It is accepted that, because input resistance of vascular smooth muscle cells is high (10^{10} ohm), very few ion channels need to be open to have substantial effect on membrane potential[24]. Therefore, it is possible that even hardly detectable activation of BK_{Ca} channel may evoke relaxation of SMC.

In line with earlier work focusing on other vascular beds[12, 35], our data in CA show that inhibitors of PDE3 and PDE4 potentiate the relaxant responses to ISO, a receptor-mediated cAMP-elevating agent, and L-85, a direct AC activator. Besides, responses to these stimulators were inhibited by IBTX, an observation consistent with previous studies[25]. Interestingly, IBTX inhibited the action of Ro and Cil only under β-AR stimulation, but not under broad AC

stimulation. This suggests that β-AR-stimulated cAMP is preferentially controlled by PDEs acting on BK_{Ca} channels, while L-85 response is impeded by PDEs acting on other effectors. This would be consistent with compartmentalization of cAMP in these cells, created by signalling domains including PDE3/4, BK_{Ca} channel and β-AR. A signalosome involving BK_{Ca} channels, β_2-AR, L-type Ca^{2+} channels and the scaffolding protein AKAP79/150, was previously characterized in VSMCs[42]. In other cell types, PDE4D was detected in a macromolecular complex involving β_2-AR whereas PDE4B was associated with the L-type Ca^{2+} channel (reviewed in Mika et al., 2012[20]). To our knowledge, there is no available evidence for localization of PDE3 isoforms in such sarcolemma complex involving β-AR. Here, we took advantage of the novel PLA technique to show that PDE3 and PDE4 isoforms are localized in the vicinity of BK_{Ca} channels in LADCA SMCs. Nevertheless, resolution of this technique is limited since two antigens as far as 40 nm from each other can generate a PLA signal. Further data supporting the existence of a macromolecular complex might be given by biochemical methods although these are challenging to use in native small arteries yielding small amount of material. Yet, our data offer new insights toward the characterization of a new signalling complex with important functional relevance in regulating arterial tone under β-AR stimulation. Since recent studies in bladder SMCs showed that PDE4 inhibition elevated BK_{Ca} activity by stimulating Ca^{2+} release[43, 44], it was of interest to address whether this coupling was relevant in vascular SMCs. Our data did not support a major role of such a mechanism in the vasorelaxant effects of Cil and Ro in unstimulated conditions. This implies that Ca^{2+} participating to BK_{Ca} activation may rather originate from Ca^{2+} influx[23].

4.2 Contribution of BK_{Ca} channel to the relaxant action of PDE3/4 inhibition is lost in HF

Importantly, by clear contrast with age-matched sham animals, BK_{Ca} channels did not mediate the relaxant effect of PDE3 and PDE4 inhibitors in arteries from HF rat. This indicates that the relaxation was mediated by other mechanisms than BK_{Ca} channels activation, which may include action on other ion channels, increased Ca^{2+} pumping, decreased Ca^{2+}-sensitivity of the myosin light chain phosphorylation, or uncoupling of contractile machinery[16]. A straightforward explanation would be that collapse of the IBTX-sensitive contribution was a direct consequence of the decrease of the amount of BK_{Ca} channel α-s.u. observed in HF-LADCA. Such a down-regulation of BK_{Ca} channel expression was previously described in mesenteric arteries from mice which developed HF following myocardial infarction[28] and in other models of cardiovascular disorders[22], and was generally associated with a reduced amount of the channel α- and/or β-s.u. Data in CA, however, are scarce: a study reported no alteration of channel expression in a rat model with cardiac hypertrophy following injection of ISO[45]. In the latter work, however, animals presented only mild remodelling, whereas the rats

studied here were submitted to chronically elevated afterload and displayed dramatic cardiac hypertrophy and lung congestion.

In parallel, we report a decrease of a ≈98 kDa PDE3A isoform, together with a marked increase in a ≈70 kDa PDE4B isoform in the HF-LADCA. Decrease in PDE3A expression was reported to be a feature of SMC switching to a proliferative phenotype[46], consistent with the intense vascular wall remodelling that was seen in the CA from HF rats. Robust increase in the 70-kDa PDE4B was also observed in aorta using the same model. Thus this alteration may constitute a hallmark of remodelling vascular tissue, at least in HF.

A limitation to our study was that contractility of LADCA from rats with HF was strikingly reduced compared to sham (Figure 4C) and this was associated with wall thickening and remodelling. In contrast, contractility was slightly increased in aortic rings from rat submitted to the same model[9]. Exposure of both vascular beds to contrasted hemodynamic stress (LADCA being upstream the stenosis whereas aorta being downstream) may explain differential alteration of contractility. Still, a milder aortic banding model in guinea pig yielded CA with thickened wall but normal active media stress[8], while septal arteries from rats with congestive HF five weeks following myocardial infarction displayed quasi-normal structure with higher response to contractile stimuli[47]. Thus loss of reactivity of CA in our study may be related to specific hemodynamic stress caused by severe stenosis rather than deterioration of myocardial function. The exact mechanisms remain to be determined and may include deleterious wall remodelling with a loss of muscular capacity. The conclusion of our study will have to be taken cautiously when extended to other forms of HF such as post-myocardial infarction and HF with preserved ejection fraction.

Coronary reserve is well known to be altered in severe cardiac hypertrophy, including in patients or animal models submitted to chronic afterload[4, 5]. The observation that combined PDE3 and PDE4 stimulation yield almost maximal relaxation of LADCA suggests that dilatory mechanisms are still functional, although the BK_{Ca} component is apparently abolished. Because our study focused on large arteries mounted on an isometric myograph, caution must be taken when extending our conclusions to *in vivo* changes in coronary reserve, which does not depend solely on vasodilatory mechanisms, but also on basal blood flow and minimal coronary resistance in the whole myocardium circulation.

4.3 Conclusion

In conclusion, this study identifies cAMP-PDE–BK_{Ca} channel coupling as a key signalling pathway for fine tuning of vascular tone (Figure 8). Our results demonstrate that the contribution of this mechanism to global tone regulation by PDEs varies depending on the

mode of cAMP stimulation and in pathophysiological context of HF. The last result may be explained by decreased expression of BK_{Ca} channel in HF. Further studies are needed to delineate the structural determinants of cyclic nucleotide compartmentation among various effectors in the vascular smooth muscle and how they are modified in disease.

5. Funding

This work was supported by the University Paris-Sud (*Attractivité* 2013 grant to B. M.); the grant [ANR-10-LABX-33] as members of the Laboratory of Excellence LERMIT; and the French Ministère de l'Enseignement et de la Recherche for a PhD fellowship awarded to S. I.

6. Acknowledgments

We are thankful to Dr Chen Yan (University of Rochester Medical Center, NY, USA), and Dr Marco Conti (University of California, San Francisco, CA, USA) for kindly providing PDE3A and PDE4A/B/D antibodies, respectively. Dr Delphine Mika, Dr Guillaume Pidoux, Dr Milia Belacel-Ouari and Dr Bertrand Crozatier are acknowledged for kindly providing expertise on specific protocols. F. Gaudin performed tissue sections and staining at the IPSIT PHIC facility at Univ. Paris-Sud.

7. Conflict of Interest

None declared.

8. References

1. Treasure CB, Vita JA, Cox DA, Fish RD, Gordon JB, Mudge GH, Colucci WS, Sutton MG, Selwyn AP, Alexander RW, Ganz P. Endothelium-dependent dilation of the coronary microvasculature is impaired in dilated cardiomyopathy. *Circulation* 1990;**81**:772-779.
2. Vatner SF, Hittinger L. Coronary vascular mechanisms involved in decompensation from hypertrophy to heart failure. *J Am Coll Cardiol* 1993;**22**:34A-40A.
3. Krams R, Kofflard MJ, Duncker DJ, Von Birgelen C, Carlier S, Kliffen M, ten Cate FJ, Serruys PW. Decreased coronary flow reserve in hypertrophic cardiomyopathy is related to remodeling of the coronary microcirculation. *Circulation* 1998;**97**:230-233.

4. Marcus ML, Doty DB, Hiratzka LF, Wright CB, Eastham CL. Decreased coronary reserve: A mechanism for angina pectoris in patients with aortic stenosis and normal coronary arteries. *N Engl J Med* 1982;**307**:1362-1366.
5. Tsai SH, Lu G, Xu X, Ren Y, Hein TW, Kuo L. Enhanced endothelin-1/Rho-kinase signalling and coronary microvascular dysfunction in hypertensive myocardial hypertrophy. *Cardiovasc Res* 2017;**113**:1329-1337.
6. Inoue T, Sakai Y, Morooka S, Hayashi T, Takayanagi K, Yamaguchi H, Kakoi H, Takabatake Y. Vasodilatory capacity of coronary resistance vessels in dilated cardiomyopathy. *Am Heart J* 1994;**127**:376-381.
7. Kiuchi K, Sato N, Shannon RP, Vatner DE, Morgan K, Vatner SF. Depressed beta-adrenergic receptor- and endothelium-mediated vasodilation in conscious dogs with heart failure. *Circ Res* 1993;**73**:1013-1023.
8. McGoldrick RB, Kingsbury M, Turner MA, Sheridan DJ, Hughes AD. Left ventricular hypertrophy induced by aortic banding impairs relaxation of isolated coronary arteries. *Clin Sci (Lond)* 2007;**113**:473-478.
9. Hubert F, Belacel-Ouari M, Manoury B, Zhai K, Domergue-Dupont V, Mateo P, Joubert F, Fischmeister R, Leblais V. Alteration of vascular reactivity in heart failure: Role of phosphodiesterases 3 and 4. *Br J Pharmacol* 2014;**171**:5361-5375.
10. Maurice DH, Ke H, Ahmad F, Wang Y, Chung J, Manganiello VC. Advances in targeting cyclic nucleotide phosphodiesterases. *Nat Rev Drug Discov* 2014;**13**:290-314.
11. Komas N, Lugnier C, Stoclet JC. Endothelium-dependent and independent relaxation of the rat aorta by cyclic nucleotide phosphodiesterase inhibitors. *Br J Pharmacol* 1991;**104**:495-503.
12. Polson JB, Strada SJ. Cyclic nucleotide phosphodiesterases and vascular smooth muscle. *Annu Rev Pharmacol Toxicol* 1996;**36**:403-427.
13. Kaneda T, Kubota T, Fujimoto K, Urakawa N, Nakajyo S, Shimizu K. Effects of rolipram on U46619-induced contraction and cyclic nucleotide content in the porcine coronary artery. *J Smooth Muscle Res* 2010;**46**:17-29.
14. Rump AF, Acar D, Klaus W. A quantitative comparison of functional and anti-ischaemic effects of the phosphodiesterase-inhibitors, amrinone, milrinone and levosimendan in rabbit isolated hearts. *Br J Pharmacol* 1994;**112**:757-762.
15. Lindgren S, Andersson KE. Effects of selective phosphodiesterase inhibitors on isolated coronary, lung and renal arteries from man and rat. *Acta Physiol Scand* 1991;**142**:77-82.
16. Morgado M, Cairrao E, Santos-Silva AJ, Verde I. Cyclic nucleotide-dependent relaxation pathways in vascular smooth muscle. *Cell Mol Life Sci* 2012;**69**:247-266.
17. White RE, Kryman JP, El-Mowafy AM, Han G, Carrier GO. cAMP-dependent vasodilators cross-activate the cgmp-dependent protein kinase to stimulate BK_{Ca} channel activity in coronary artery smooth muscle cells. *Circ Res* 2000;**86**:897-905.
18. Roberts OL, Kamishima T, Barrett-Jolley R, Quayle JM, Dart C. Exchange protein activated by cAMP (EPAC) induces vascular relaxation by activating Ca^{2+}-sensitive K^+ channels in rat mesenteric artery. *J Physiol* 2013.
19. Stott JB, Barrese V, Greenwood IA. K_V7 channel activation underpins EPAC-dependent relaxations of rat arteries. *Arterioscler Thromb Vasc Biol* 2016;**36**:2404-2411.
20. Mika D, Leroy J, Vandecasteele G, Fischmeister R. PDEs create local domains of cAMP signaling. *J Mol Cell Cardiol* 2012;**52**:323-329.
21. Wu RS, Marx SO. The BK potassium channel in the vascular smooth muscle and kidney: alpha- and beta-subunits. *Kidney Int* 2010;**78**:963-974.
22. Hu XQ, Zhang L. Function and regulation of large conductance Ca^{2+}-activated K^+ channel in vascular smooth muscle cells. *Drug Discov Today* 2012;**17**:974-987.

23. Latorre R, Castillo K, Carrasquel-Ursulaez W, Sepulveda RV, Gonzalez-Nilo F, Gonzalez C, Alvarez O. Molecular determinants of BK channel functional diversity and functioning. *Physiol Rev* 2017;**97**:39-87.
24. Nelson MT, Cheng H, Rubart M, Santana LF, Bonev AD, Knot HJ, Lederer WJ. Relaxation of arterial smooth muscle by calcium sparks. *Science* 1995;**270**:633-637.
25. Price JM, Cabell JF, Hellermann A. Inhibition of camp mediated relaxation in rat coronary vessels by block of Ca^{2+} activated K^+ channels. *Life Sci* 1996;**58**:2225-2232.
26. Porter VA, Bonev AD, Knot HJ, Heppner TJ, Stevenson AS, Kleppisch T, Lederer WJ, Nelson MT. Frequency modulation of Ca^{2+} sparks is involved in regulation of arterial diameter by cyclic nucleotides. *Am J Physiol* 1998;**274**:C1346-1355.
27. Wellman GC, Nathan DJ, Saundry CM, Perez G, Bonev AD, Penar PL, Tranmer BI, Nelson MT. Ca^{2+} sparks and their function in human cerebral arteries. *Stroke* 2002;**33**:802-808.
28. Wan E, Kushner JS, Zakharov S, Nui XW, Chudasama N, Kelly C, Waase M, Doshi D, Liu G, Iwata S, Shiomi T, Katchman A, D'Armiento J, Homma S, Marx SO. Reduced vascular smooth muscle BK channel current underlies heart failure-induced vasoconstriction in mice. *FASEB J* 2013;**27**:1859-1867.
29. Feldman AM, Weinberg EO, Ray PE, Lorell BH. Selective changes in cardiac gene expression during compensated hypertrophy and the transition to cardiac decompensation in rats with chronic aortic banding. *Circ Res* 1993;**73**:184-192.
30. Thompson WJ, Appleman MM. Multiple cyclic nucleotide phosphodiesterase activities from rat brain. *Biochemistry* 1971;**10**:311-316.
31. Nyborg NC, Baandrup U, Mikkelsen EO, Mulvany MJ. Active, passive and myogenic characteristics of isolated rat intramural coronary resistance arteries. *Pflugers Arch* 1987;**410**:664-670.
32. Singer JJ, Walsh JVJ. Characterization of calcium-activated potassium channels in single smooth muscle cells using the patch-clamp technique. *Pflugers Arch* 1987;**408**:98-111.
33. White RE, Darkow DJ, Lang JL. Estrogen relaxes coronary arteries by opening BK_{Ca} channels through a cgmp-dependent mechanism. *Circ Res* 1995;**77**:936-942.
34. Maurice DH, Crankshaw D, Haslam RJ. Synergistic actions of nitrovasodilators and isoprenaline on rat aortic smooth muscle. *Eur J Pharmacol* 1991;**192**:235-242.
35. Bardou M, Goirand F, Bernard A, Guerard P, Gatinet M, Devillier P, Dumas JP, Morcillo EJ, Rochette L, Dumas M. Relaxant effects of selective phosphodiesterase inhibitors on U46619 precontracted human intralobar pulmonary arteries and role of potassium channels. *J Cardiovasc Pharmacol* 2002;**40**:153-161.
36. Rieg AD, Rossaint R, Verjans E, Maihofer NA, Uhlig S, Martin C. Levosimendan relaxes pulmonary arteries and veins in precision-cut lung slices - the role of K-channels, cAMP and cGMP. *PLoS One* 2013;**8**:e66195.
37. Li H, Hong da H, Son YK, Na SH, Jung WK, Bae YM, Seo EY, Kim SJ, Choi IW, Park WS. Cilostazol induces vasodilation through the activation of Ca^{2+}-activated K^+ channels in aortic smooth muscle. *Vascul Pharmacol* 2015;**70**:15-22.
38. Khanamiri S, Soltysinska E, Jepps TA, Bentzen BH, Chadha PS, Schmitt N, Greenwood IA, Olesen SP. Contribution of K_v7 channels to basal coronary flow and active response to ischemia. *Hypertension* 2013;**62**:1090-1097.
39. Mani BK, Robakowski C, Brueggemann LI, Cribbs LL, Tripathi A, Majetschak M, Byron KL. $K_v7.5$ potassium channel subunits are the primary targets for PKA-dependent enhancement of vascular smooth muscle K_v7 currents. *Mol Pharmacol* 2016;**89**:323-334.

40. Sudo T, Tachibana K, Toga K, Tochizawa S, Inoue Y, Kimura Y, Hidaka H. Potent effects of novel anti-platelet aggregatory cilostamide analogues on recombinant cyclic nucleotide phosphodiesterase isozyme activity. *Biochem Pharmacol* 2000;**59**:347-356.

41. Liu G, Shi J, Yang L, Cao L, Park SM, Cui J, Marx SO. Assembly of a Ca^{2+}-dependent BK channel signaling complex by binding to beta2 adrenergic receptor. *EMBO J* 2004;**23**:2196-2205.

42. Xin W, Li N, Cheng Q, Petkov GV. BK channel-mediated relaxation of urinary bladder smooth muscle: A novel paradigm for phosphodiesterase type 4 regulation of bladder function. *J Pharmacol Exp Ther* 2014.

43. Zhai K, Chang Y, Wei B, Liu Q, Leblais V, Fischmeister R, Ji G. Phosphodiesterase types 3 and 4 regulate the phasic contraction of neonatal rat bladder smooth myocytes via distinct mechanisms. *Cell Signal* 2014;**26**:1001-1010.

44. Kim N, Chung J, Kim E, Han J. Changes in the Ca^{2+}-activated K^+ channels of the coronary artery during left ventricular hypertrophy. *Circ Res* 2003;**93**:541-547.

45. Dunkerley HA, Tilley DG, Palmer D, Liu H, Jimmo SL, Maurice DH. Reduced phosphodiesterase 3 activity and phosphodiesterase 3A level in synthetic vascular smooth muscle cells: Implications for use of phosphodiesterase 3 inhibitors in cardiovascular tissues. *Mol Pharmacol* 2002;**61**:1033-1040.

46. Stassen FR, Fazzi GE, Leenders PJ, Smits JF, De Mey JG. Coronary arterial hyperreactivity and mesenteric arterial hyporeactivity after myocardial infarction in the rat. *J Cardiovasc Pharmacol* 1997;**29**:780-788.

9. Figure Legends

Figure 1. BK_{Ca} channel inhibition inhibited the relaxant effect of cAMP-PDE inhibitors in rat LADCA. Selective PDE4 inhibitor (Ro, 10 µmol/L), or PDE3 inhibitor (Cil, 1 µmol/L), or both inhibitors were applied on LADCA rings contracted with U46619 (U46, 0.3-3 µmol/L) in the presence of BK_{Ca} channel inhibitor IBTX (**A**, **B**, **C**, 0.1 µmol/L), various ion channel inhibitors (**D**) or relevant vehicle (veh., **A-D**). **A:** Examples of traces obtained in the absence (veh., left-hand side) or in the presence of IBTX (right-hand side). **B:** Scatter plot showing individual data points and mean relaxation ± SEM, in percentage of initial contraction. (+): IBTX; (-): Control. **C:** Relaxant effect by Ro + Cil was still inhibited by IBTX in rings after the endothelium was voluntarily damaged ($endo^{(-)}$). **D:** Relaxant effect of combined application of Ro and Cil was not altered by either ryanodine (30 µmol/L), glibenclamide (glib.,10 µmol/L), DPO-1 (1 µmol/L), or STX (0.1 µmol/L), but was reduced by XE991 (30 µmol/L). Shown are individual data and means ± SEM. N=5-13. **: P<0.01, ***: P<0.001 (Mann-Whitney test). ###: P≤0.001 (ANOVA followed by Holm-Sidak's multiple comparison test).

Figure 2. Ro (10 µmol/L) together with Cil (1 µmol/L) increased NP_o, mean open time and NF_o of BK_{Ca} channels in LADCA SMCs. Both inhibitors had no significant effect when used alone. **A:** Data from 3 independent cell-attached patches are shown, during DMSO perfusion (**a**, **b** and **c**) and during Ro+Cil perfusion of the same cells (**a', b'** and **c'**, respectively). Patch potential was 40 mV. NP_o associated to the displayed traces are indicated. Amplitude histograms generated from the whole analysed period in each condition are also shown. **B-D:** Summary individual (grey dots) and mean±SEM (black lines) data of NP_o (**B**), mean open time (**C**) and opening frequency (NF_o, **D**) are presented. n=5-11 cells from N=5-7 rats. *: P<0.05 vs. DMSO (Wilcoxon signed-rank test performed on means per rat).

Figure 3. Effect of PDE4 or PDE3 inhibition on concentration-response curves to isoprenaline or L-858051 in LADCA rings. PDE4 (Ro, 10 µmol/L: **A, B, E, F**) or PDE3 (Cil 1 µmol/L: **C, D, G, H**) inhibition was tested on CRCs to isoprenaline (ISO, **A-D**) or L-858051 (L-85, **E-H**) in LADCA rings incubated with IBTX, in the right panels, or relevant vehicle, in the left panels. In the right panels (**B, D, F, H**), dashed line represents the CRC fit from control data. N=6-14. ***: P<0.001 (2-way ANOVA for repeated measures).

Figure 4. Rats with aortic stenosis exhibit signs of heart failure, remodelling of the wall of large coronary arteries and altered vasoreactivity of LADCA. A: Summary values of organ weight over tibia length (TL) ratios for heart, lung, kidney and liver, as well as body weight from sham rats and rats with aortic stenosis included for LADCA isolation and histology (HF; lung weight/TL >650 mg/cm). N=23-26; $$$: P<0.001, Welsh's t-test). **B:** Representative

left ventricle cross-sections from sham and HF rats stained with Masson trichrome, displaying large arteries. The scatter plot represents quantification of [wall/vessel diameter] ratio in large arteries (n=22-23 from N=3 rats per group; #: P<0.05, nested ANOVA). **C-D: Vasoreactivity** in LADCA from sham and HF rats: contractile response to K80 and 1 µmol/L U46619 (C; N=7 rats) and relaxant response to ACh (D; N=7 rats). **: P<0.01, ***: P<0,001 (Mann-Whitney test); §§§: 2-way ANOVA for repeated measures. Plots show mean values ± SEM.

Figure 5. BK_{Ca} channel inhibition has no effect on the relaxant effect of PDE3/4 inhibitors in HF-LADCA. PDE4 inhibitor (**A**, Ro, 10 µmol/L), PDE3 inhibitor (**B**, Cil, 1 µmol/L) or both inhibitors (**C**) were applied on U46619-contracted (1-3 µmol/L) LADCA rings from sham and HF rats in the presence of IBTX (+) or vehicle (-). Scatter plot showing individual data points and mean relaxation ± SEM, in percentage of initial contraction. N=4-7. *: P<0.05, **: P<0.01 (2-way ANOVA followed by Holm-Sidak test). In **B**, effect of Cil was overall significantly higher in HF compared with sham (P ≤ 0.01, 2-way ANOVA).

Figure 6. Expression of BK_{Ca} and PDE proteins in sham and HF rat LADCA. Expression of BK_{Ca} α-s.u. (**A**), PDE3A, PDE4A, PDE4B and PDE4D (**B**, from left to right, respectively) proteins in LADCA isolated from sham or HF rats. Representative immunoblots obtained for these proteins and matching GAPDH signal are shown. Arrows indicate the bands that were quantified. Scatter plots show individual values and mean ± SEM from relative densitometric quantification normalized to GAPDH and averaged signal in sham. N=5 for BK_{Ca} α-s.u. and PDE4B, N=9 for PDE3A, N=6 for PDE4A and N=4 for PDE4D. *: P<0.05, **: P<0.01 (Mann and Whitney test).

Figure 7. Evidence for PDE3/4-BK_{Ca} α-subunit signals. PLA using an antibody against BK_{Ca} α-subunit associated with anti-PDE3A (**A**), anti-PDE4 (pan specific, **B**) or anti-PDE4B (**C**) antibody in sham- (images in upper panel, empty circles in scatter plot) or HF- (images in middle panel, filled circles) LADCA SMCs. Representative images are shown. Scale bar: 5 µm. Inset shows transmitted light image. Plots in lower panels show respective quantifications of PLA signal (individual data and mean ± SEM) of n=12-84 cells from 2-3 rats.

Figure 8. Schematic representation of the differential contribution of BK_{Ca} channels to the relaxant effects of PDE3 and PDE4 inhibitors in rat LADCA. A. Under basal cAMP production rate, Ro and Cil produce a relaxation in which the BK_{Ca} channels play essential role. K^+ channels limit depolarization of cell membrane potential, resulting in closing L-type Ca^{2+} channels (LTCC), reduction of intracellular calcium concentration ($[Ca^{2+}]_i$) and relaxation. This would be facilitated by proximity of PDE3 and PDE4 isoforms with the channel. K_V7 channels

also participate in the action of PDE inhibitors. **B.** Under stimulation of cAMP production *via* the β-AR (ISO), Ro and Cil action depends mostly on coupling with BK_{Ca} channels. Under broad stimulation of the AC with L-85, participation of the channel is not apparent, and other effectors may mediate the relaxation. **C.** In LADCA from rats with heart failure, participation of the channel to the relaxant action of Ro and Cil is absent, in contrast with sham. Variation of expression of BK_{Ca} (🡻), short form of PDE3A (🡻) and PDE4B (🡹) proteins are shown.

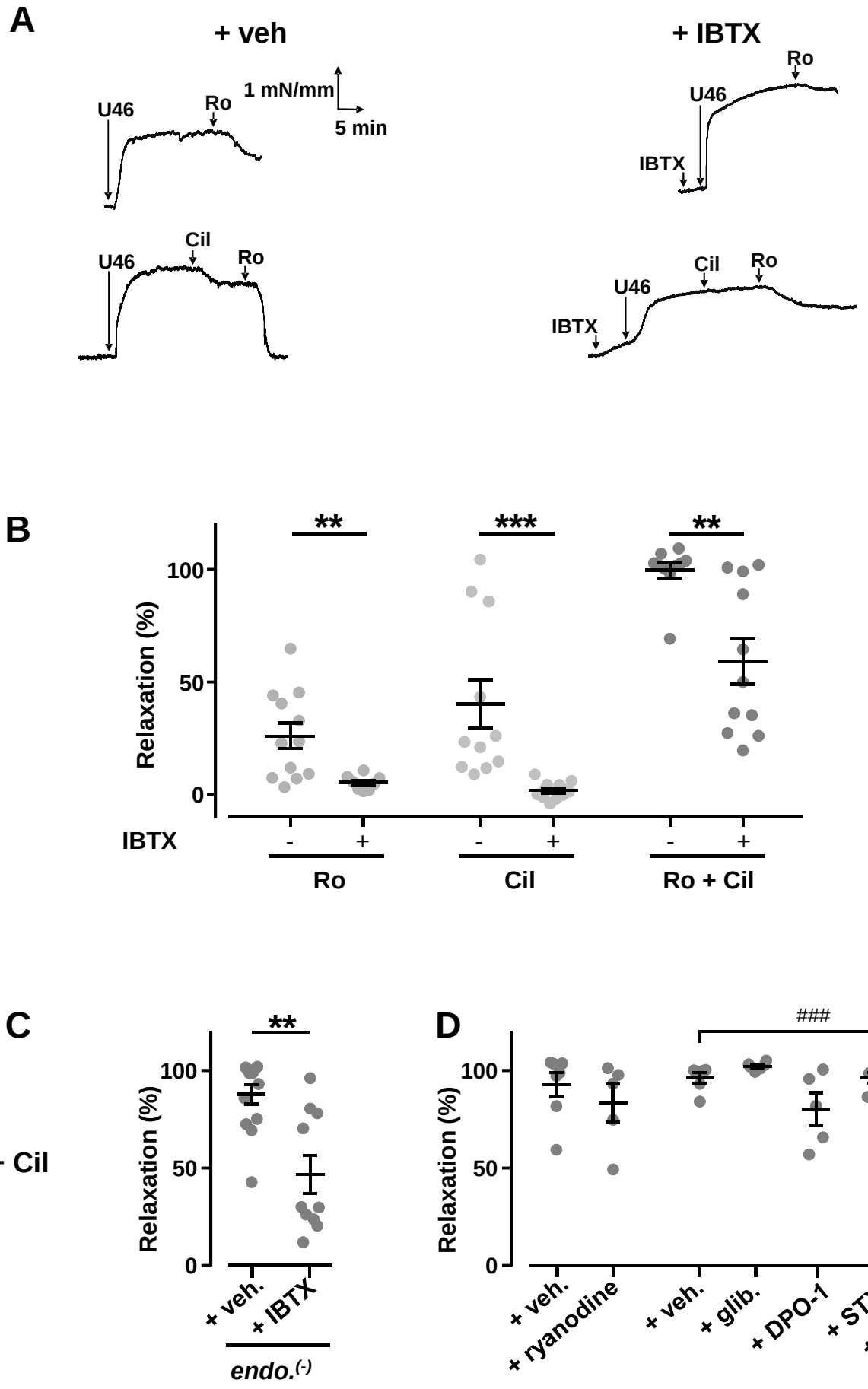
A
+ veh
+ IBTX
1 mN/mm
5 min
U46
Ro
Cil
IBTX
B
Relaxation (%)
100
50
0
**
***
**
IBTX
-
+
Ro
Cil
Ro + Cil
C
Ro + Cil
Relaxation (%)
**
+ veh.
+ IBTX
endo.(-)
D
###
+ veh.
+ ryanodine
+ glib.
+ DPO-1
+ STX
+ XE991

Figure 1

Figure 2

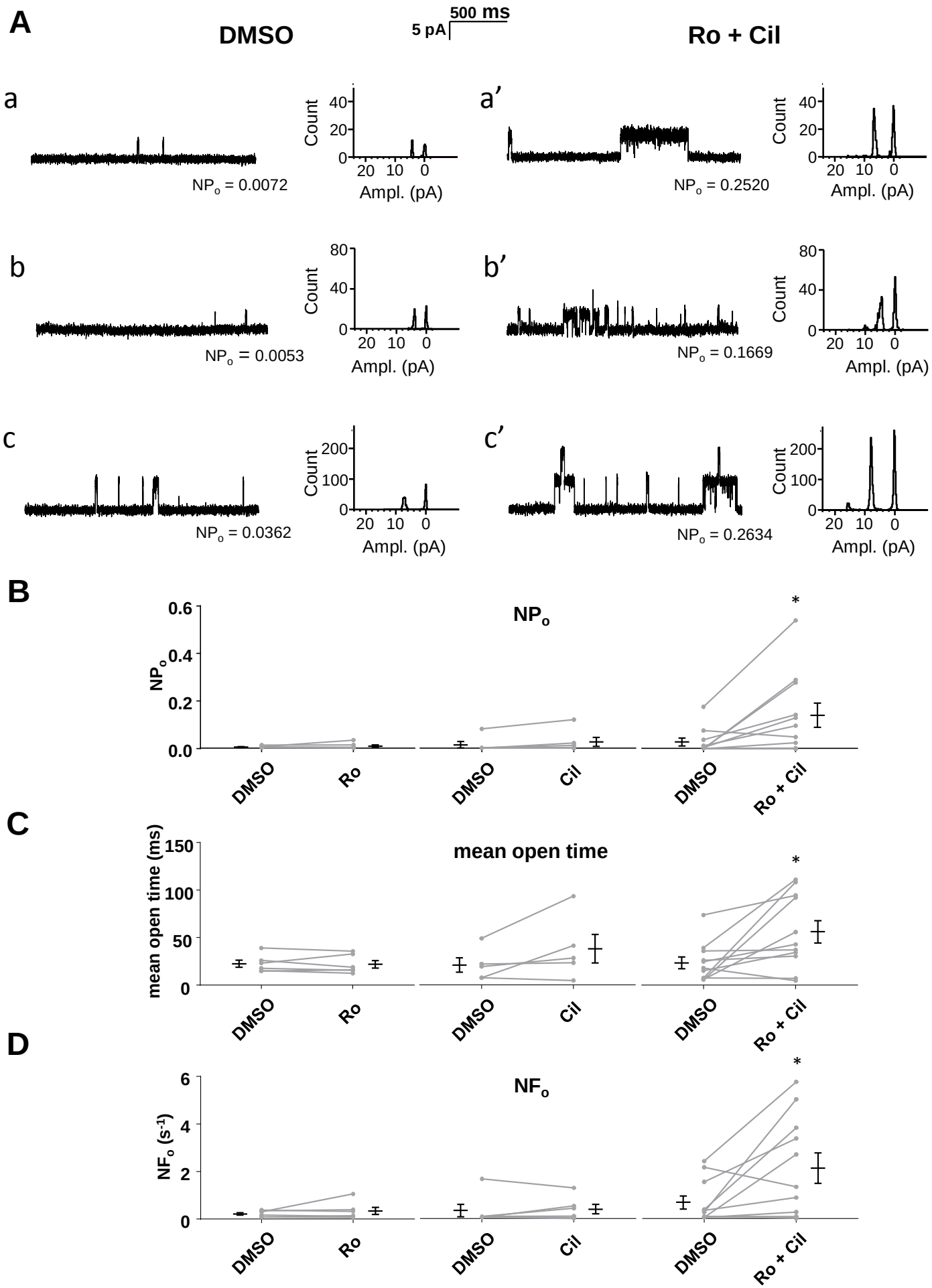

Figure 2

Figure 3

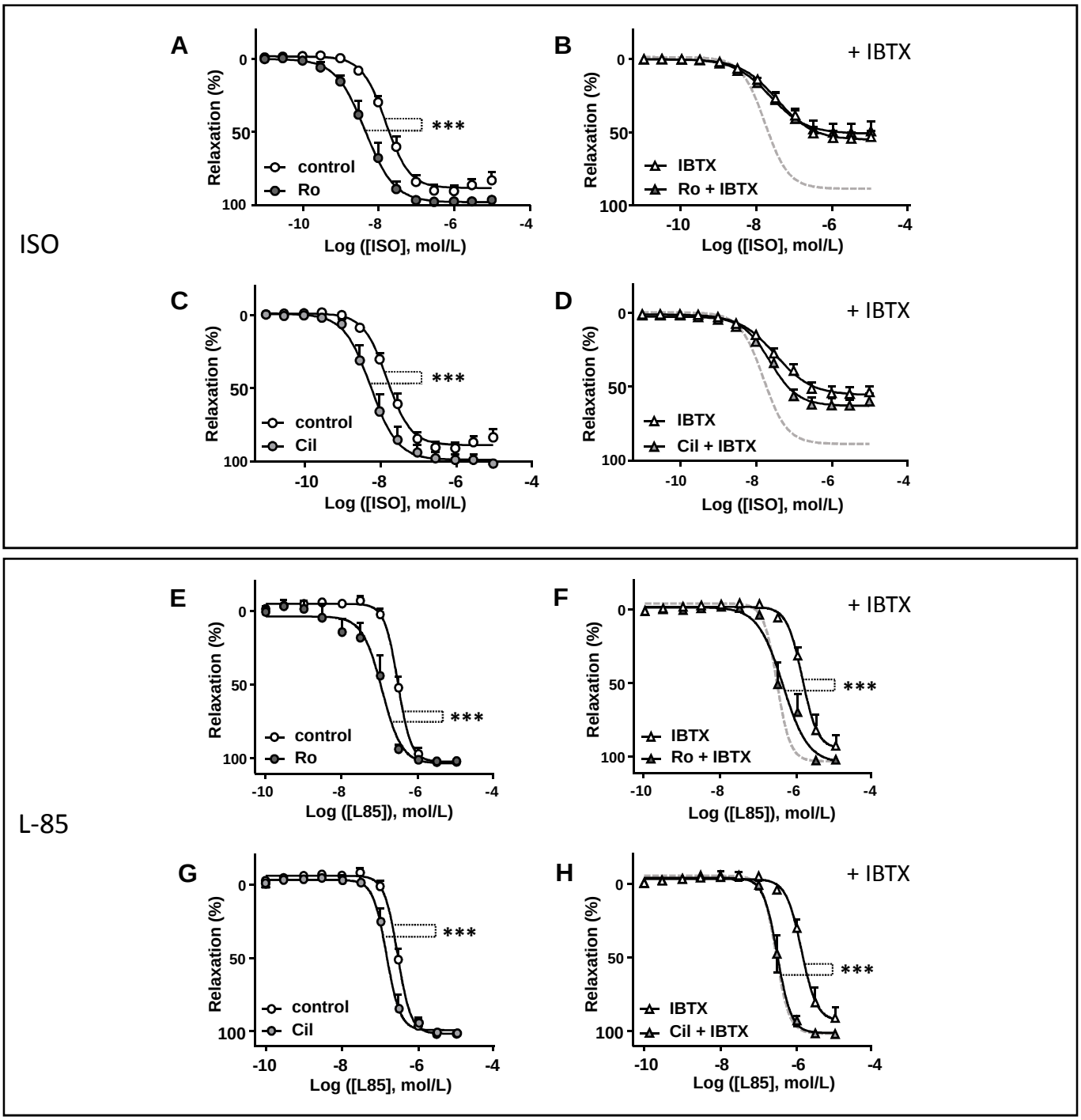

Figure 3

Figure 4

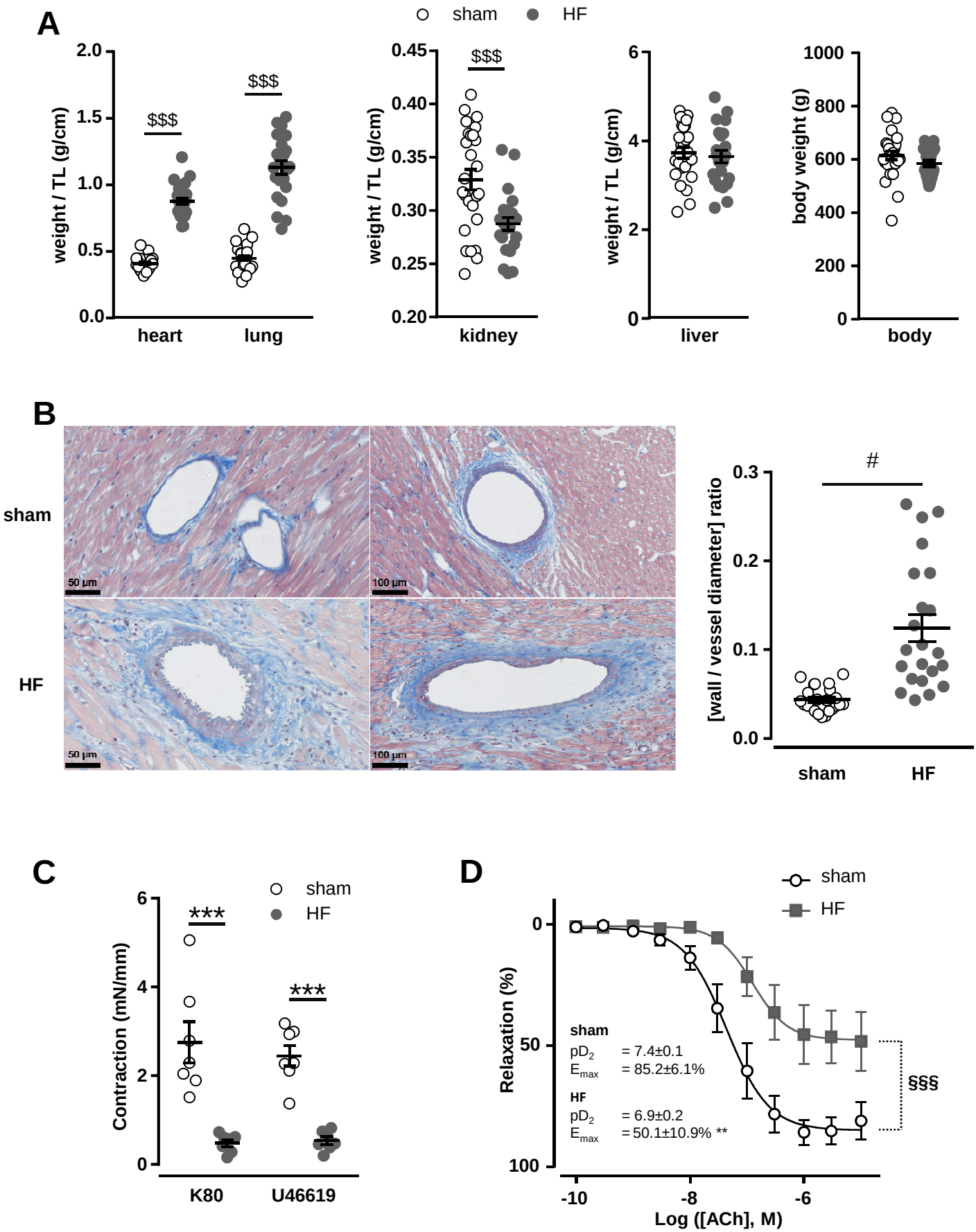

Figure 4

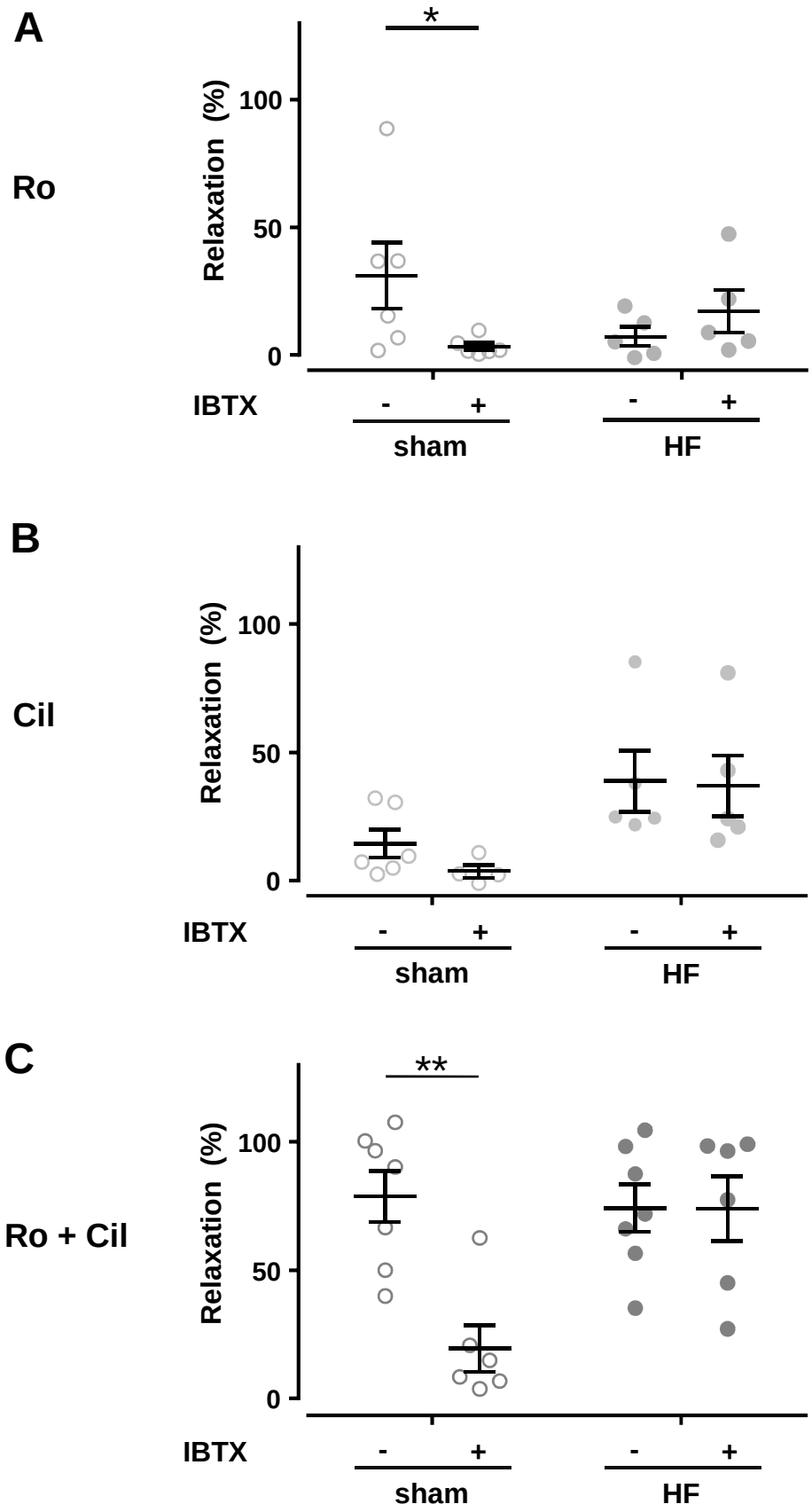
A
Ro
*
Relaxation (%)
100
50
0
IBTX
-
+
-
+
sham
HF
B
Cil
Relaxation (%)
100
50
0
IBTX
-
+
-
+
sham
HF
C
Ro + Cil
**
Relaxation (%)
100
50
0
IBTX
-
+
-
+
sham
HF

Figure 5

Figure 6

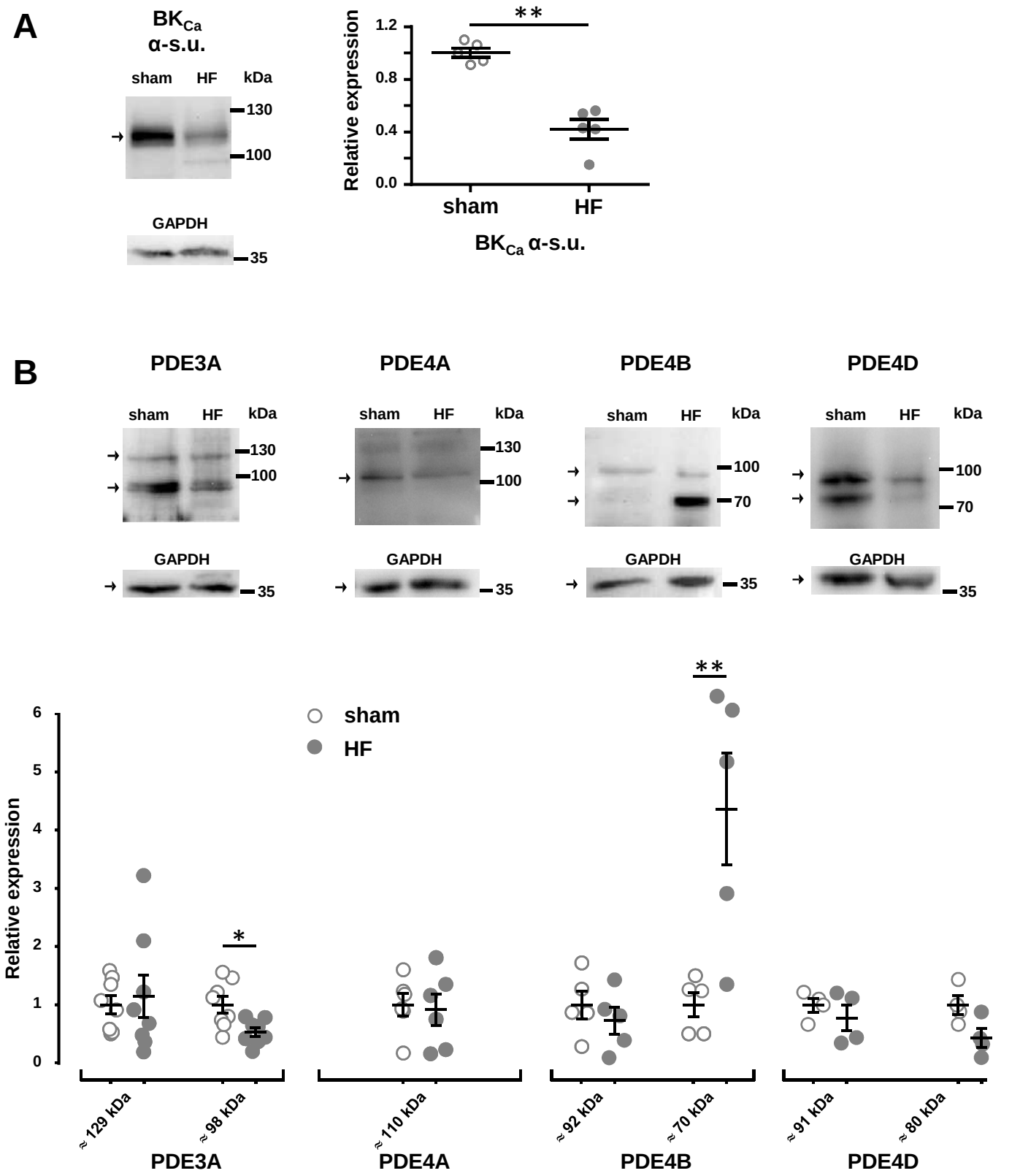

Figure 6

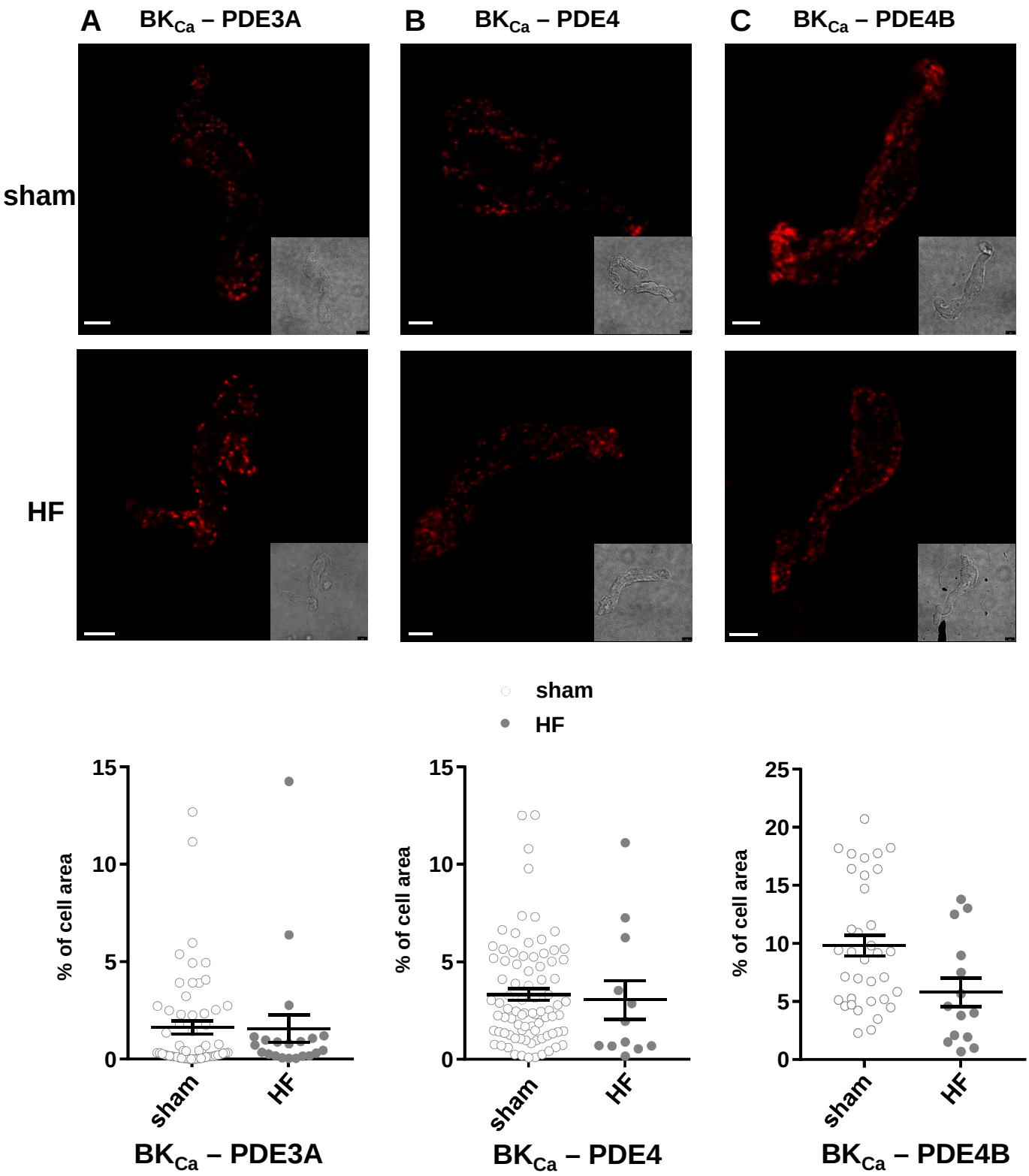
A
BKCa – PDE3A
B
BKCa – PDE4
C
BKCa – PDE4B
sham
HF
sham
HF
% of cell area
15
10
5
0
sham
HF
BKCa – PDE3A
% of cell area
15
10
5
0
sham
HF
BKCa – PDE4
% of cell area
25
20
15
10
5
0
sham
HF
BKCa – PDE4B

Figure 7

Figure 8

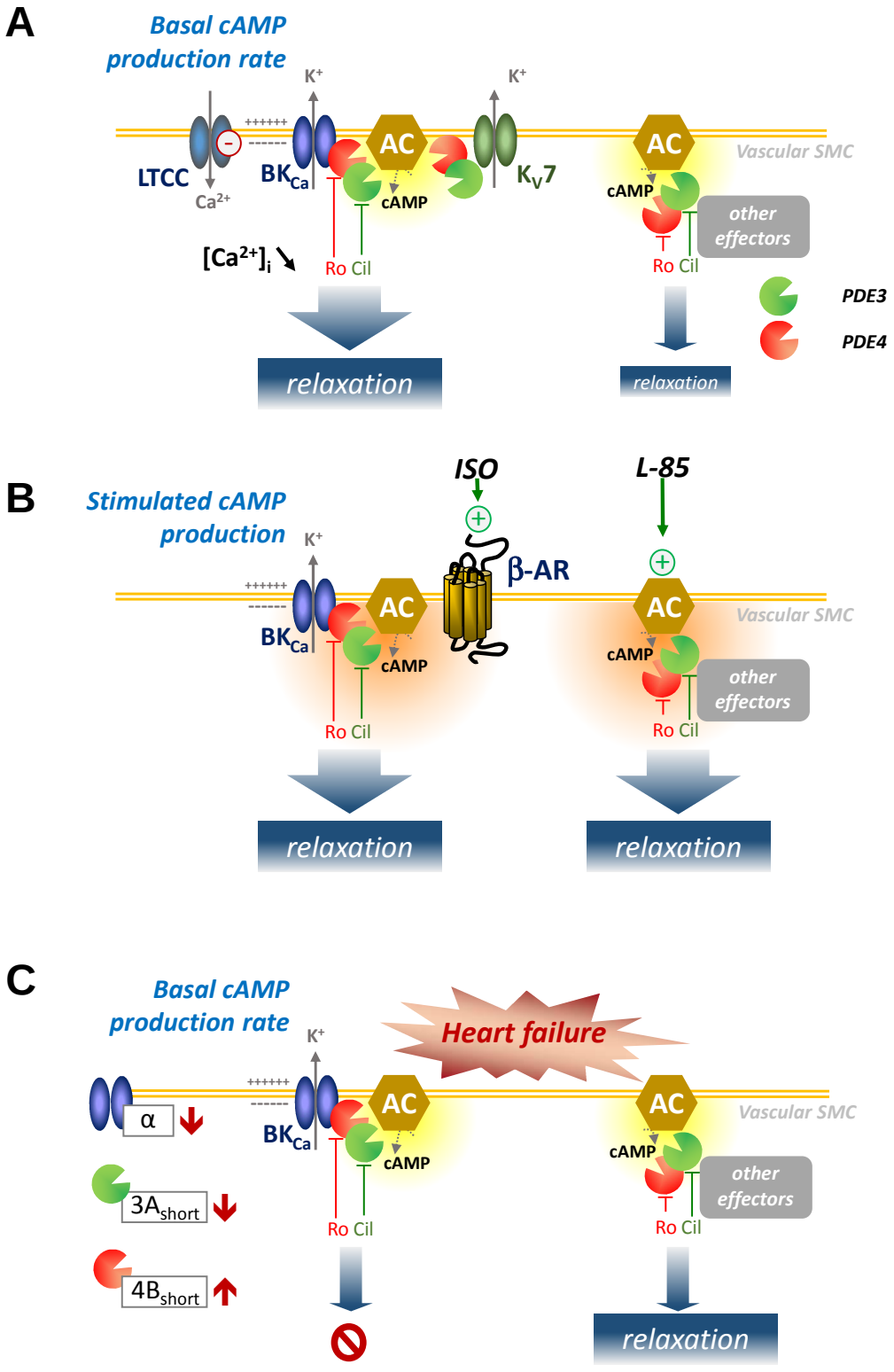

Figure 8

SUPPLEMENTARY MATERIAL

CONTENTS

1. Detailed Material and Methods

1.1 Animals and surgical procedures

All animal care and experimental procedures conformed to the European Community guiding principles in the care and use of animals (Directive 2010/63/EU of the European Parliament) and authorizations to perform animal experiments according to application decrees were obtained from the French Ministry of Agriculture, Fisheries and Food (No. C92-019-01, 03 August 2016). A total of 164 rats were used in the experiments described here. This included 8-12-week-old, male Wistar rats that were used for basic physiological exploration. In addition, 37 rats with HF sacrificed 22 weeks after surgical stenosis of the ascending aorta were used. The surgical procedure was carried out on 3-week-old rats, under anaesthesia with a ketamine-xylazine mix (75 mg/kg – 10 mg/kg, respectively, 0.3 mL/100g, i.p.). Aortic stenosis was mimicked by placing a stainless steel hemoclip (0.6 mm-internal diameter) on the ascending aorta via thoracic incision, as previously described[1, 2]. Also, 32 age-matched control animals underwent the same procedure without placement of the clip. Buprenorphine chlorhydrate (0.2 mL/100g, s.c.) was administered twice daily for 3 days beginning at the end of the surgery.

Echocardiography was performed at 22 weeks after surgery on 11 SHAM-operated and 14 stenosed rats using a 12 MHz transducer (Vivid 7, General Electric Healthcare). Anaesthesia was induced and maintained using 3% and 1.5% isoflurane, respectively. Two-dimensional-guided (2D) M-mode echocardiography was used to determine wall thickness and left ventricular chamber diameter at systole and diastole, and contractile parameters such as fractional shortening and ejection fraction. Left ventricular mass (LVM, mg) was calculated according to the Penn formula home-adapted for the rat heart:

$$LVM = 1.04\,.\,(IVSd + LVIDd + LVPWd)^{3} - LVIDd^{3},$$

with IVSd: end-diastolic interventricular septum thickness; LVIDd: end-diastolic LV internal diameter; LVPWd: end-diastolic LV posterior wall thickness[3]. Volume (V) of the left ventricular chamber was evaluated using the Teicholz formula:

$$V = \frac{7D^{3}}{2.4+D},$$

where D is the diameter of the chamber[4].

1.2 Materials

Cilostamide (Cil) was purchased from Tocris Bioscience (Bristol, UK) and Ro-20-1724 (Ro) from Calbiochem (Merck Chemicals Ltd, Nottingham, UK). 3-isobutyl-1-methylxanthine (IBMX), acetylcholine (ACh), isoprenaline (ISO) phentolamine, trypsin inhibitor (T6522), bovine serum albumin, dithiothreitol (DTT), glibenclamide and snake venom from *Crotalus atrox* were supplied by Sigma Aldrich (Saint Quentin-Fallavier, France). Iberiotoxin (IBTX), a selective blocker of BK_{Ca} channels[5], was bought from Latoxan (Valence, France) or Smartox Biotechnologie (Saint Martin d'Hères, France), ryanodine and stromatoxin-1 (STX) from Alomone (Jerusalem, Israel), U46619 and XE991 from Interchim (Montluçon, France) and L-858051 (L-85) from Enzo Life Science (Villeurbanne, France). Diphenyl phosphine oxide-1 (DPO-1) was purchased from SantaCruz Biotechnology (Dallas, TX, USA).

Ro, Cil, ryanodine, glibenclamide and DPO-1 were dissolved in dimethylsulfoxyde (DMSO). Final concentration of DMSO usually did not exceed 0.03%, except for experiments using ryanodine where maximal DMSO amounted to 0.33%. ISO was prepared in ascorbic acid (1%). Other pharmacological agents were dissolved in water. For each given experiment, amounts of vehicle (water or DMSO) were matched in all groups studied. The following enzymes were used for tissue digestion: papain (Sigma Aldrich, P4762), collagenase H (Roche, 1074032 or Sigma Aldrich, C7926). All salts for solutions were from Sigma-Aldrich or Euromedex (Souffelweyersheim, France)

1.3 Coronary artery isolation and smooth muscle cells preparation

Rats were anesthetized by injection of pentobarbital (150 mg/kg, i.p.). The heart was quickly isolated and placed in an ice-cold "Krebs" solution of following composition (in mmol/L): NaCl 119, KCl 4.7, $CaCl_2(H_2O)_2$ 2.5, $MgSO_4(H_2O)_7$ 1.2, KH_2PO_4 1.2, glucose 11, $NaHCO_3$ 25, bubbled with 95% O_2 and 5% CO_2 to maintain pH at 7.4. The heart was then pinned in a Sylgard®-coated dish filled with Krebs solution and the ventricle was carefully dissected to isolate the left anterior descending coronary artery (LADCA, inner diameter 100–300 µm). Dissecting solution was renewed every 10-15 min with cold, bubbled solution. Collected tissue was then frozen in liquid nitrogen and stored at -80°C, or freshly processed, according to the following relevant protocols.

For isometric tension measurements, LADCA was cut into small segments of (0.5-2 mm length and mounted on a wire myograph (see relevant section below).

Isolated smooth muscle cells were obtained as described previously[6], with some minor modifications. Briefly, LADCA was placed into ice-cold dissociation medium (DM) composed

of (in mmol/L): NaCl 110, KCl 5, Hepes 10, KH_2PO_4 0.5, $NaHCO_3$ 0.5, taurine 10, EDTA 0.5, Glucose 10, $CaCl_2$ 0.2, $MgCl_2$ 2, pH≈7. Then tissue was incubated in papain 1.5 mg/mL in DM for 1 h, then during 6 min at 37°C in the presence of DTT (1 mg/mL) under gentle agitation. LADCA was then transferred in DM mixture containing collagenase (1.6 mg/mL) and trypsin inhibitor (1.6 mg/mL) and further incubated at 37°C for 4 min. Tissue was then washed 3 times with ice-cold DM and gently triturated using a blunt Pasteur pipette to obtain relaxed, spindle-shaped SMCs. Undigested tissue was discarded, cells were centrifugated (200 *g,* 4°C, 5 min), re-suspended in ≈0.5 mL DM and kept on ice. For patch-clamp experiments, a similar protocol was used except that only 13 min papain digestion step was performed in DTT and bovine serum albumin (1 mg/mL). Cells were used within 7 h following digestion.

1.4 cAMP-PDE activity assay

cAMP-PDE activity was measured by a two-step radioenzymatic assay according to the method reported by Thompson and Appleman[7]. Frozen LADCA were homogenized in lysis buffer containing Hepes 20 mmol/L, NaCl 150 mmol/L, EDTA 2 mmol/L, NP-40 0.5% and microcystin 1 µmol/L. During the first step, protein extracts (10 µg) were incubated in a mix containing 10 mmol/L Tris-HCl (pH=8), 10 mmol/L $MgCl_2$, 5 mmol/L β-mercaptoethanol, 1 µmol/L cAMP (Sigma Aldrich), and 10^5 cpm of [^{3}H]-cAMP (PerkinElmer, Villebon-sur-Yvette, France) for 25 min at 33°C. The reaction was performed in a final volume of 200 µL and allowed the cAMP hydrolysis by PDEs into 5'-adenosine monophosphate. The reaction was stopped by addition of 200 µL of "stop" solution (Tris-HCl 40 mmol/L, EDTA 10 mmol/L, pH=8) and boiling during 1 min. In the second step, an excess of 5'-nucleotidase (snake venom from *Crotalus atrox*, 1 mg/mL) was incubated with samples (20 min, 33°C) to convert 5' adenosine monophosphate into adenosine. The enzymatic reaction products were separated by anion-exchange chromatography using 1 mL of AG1-X8 resin (Bio-Rad, Marnes-la-Coquette, France) and quantified by scintillation counter. Reactions were carried out with or without inhibitors of PDEs, namely 100 µmol/L IBMX, as a non-selective PDE inhibitor, 1 µmol/L Cil, as a selective PDE3 inhibitor[8] and 10 µmol/L Ro, as a selective PDE4 inhibitor[9]. IBMX-sensitive PDE activity, PDE3 and PDE4 activities were defined as the fraction of total activity that was sensitive to corresponding inhibitor.

1.5 Vascular reactivity measurement

Each small segment of LADCA was mounted in the chamber of a small vessel myograph (620 M, Danish Myo Technology A/S, Aarhus, Denmark) using 25 µm tungsten wire, as previously described[10]. Chambers were filled with Krebs solution, (see above "Coronary artery isolation and smooth muscle cells preparation" for composition), bubbled with 95% O_2 - 5% CO_2 mixture and warmed at 37°C. Data were digitized using a Powerlab 8/30 (AD Instruments, Paris, France) and acquired using the Labchart7 software (AD Instruments).Vessels underwent a normalization procedure which consisted in stretching the vessels stepwise to construct tension-circumference relationship. Rings were eventually set at an internal circumference corresponding to 90% of the circumference the vessel would have if submitted to a transmural pressure of 100 mmHg (13.3 kPa). After an equilibration period of 45-60 min, contractile capacity of the vessels was evaluated by challenging them with a modified Krebs solution containing 80 mmol/L KCl with equimolar substitution of NaCl. This depolarizing solution (K80) normally evoked robust contraction, and was left for 5 min. Then chambers were washed with a "Ca^{2+}-free" modified-Krebs solution, containing no Ca^{2+} and supplemented with 0.1 mmol/L EGTA (Sigma-Aldrich), until the vessel was full relaxed and tension was stabilized. This allowed to suppress possible constitutive tone that would otherwise mask the minimum tension level. Then, normal Krebs solution was added for 5 min, "Ca^{2+}-free" modified-Krebs solution was subsequently added for 3 min and K80 challenge was repeated. After an additional series of washes, the vessels were bathed in Krebs and used for various pharmacological protocols: (i) Endothelial function was evaluated in all vessels by measurement of the relaxant effect induced by 1 µmol/L ACh following contraction of the vessels with the thromboxane A_2 mimetic U46619 (0.3- 3 µmol/L), so as to obtain a response as close as possible to the ΔK80 response. In experiments involving 8-12-week-old rats, vessels relaxing less than 50% to ACh were excluded. (ii) In experiments set out to study the vasorelaxant effect of PDE3 inhibition, the rings were contracted with U46619 (0.3 – 3 µmol/L). Once stabilized contraction was obtained, 1 µmol/L Cil (a concentration selective for PDE3 inhibition, Table S1) was added. To study additional effect of PDE4 inhibition, PDE4 inhibitor Ro (10 µmol/L, Table S1) was added on top of Cil. In other vessels, Ro was applied first and Cil was then added on the top. Data mentioned as "Cil + Ro" represented pooled data obtained using both sequences of compound addition. When addressing the role of ion channels in the relaxant effect of PDE inhibitors, inhibitors or relevant vehicle were applied during 10 min before contracting the vessels. (iii) In other experiments, vasorelaxant agonists (ACh, ISO, L-85) were added on U46619-contracted vessels in a stepwise, cumulative fashion to establish concentration-response curve (CRC). ISO was added in the presence of the α-adrenergic receptor antagonist phentolamine (10^{-5} M). Again, when relevant, Cil, Ro or IBTX were added at least 10 min before contraction.

Contractile responses were expressed in mN/mm and relaxant responses were expressed in %, relative to the contraction amplitude obtained with U46619. Tension level at the end of the last "Ca^{2+}-free" challenge was considered to be the minimal tension from which amplitude of the response was calculated.

1.6 Patch clamp

Single channel recording was performed in freshly isolated LADCA myocytes, using either cell-attached or inside-out configurations of the patch clamp technique[11]. Patch pipette, made from glass capillaries (Vitrex Medical A/S, Herlev, Denmark) pulled using a DMZ-universal puller (Zeitz-Instruments Vertriebs GmbH, Martinsried, Germany), had resistance of 2-5 MOhm. Cells suspended in ≈50 µL DM were allowed to settle 5-10 min on the bottom of a Petri dish and then gently covered by ≈3 mL of extracellular bath solution[12] (in mmol/L: KCl 140, $MgCl_2$ 10, $CaCl_2$ 0.1, Hepes 10, D-glucose 30, pH=7.2). High K^+ concentration in the bath was used to bring cell membrane potential close to 0 mV and therefore to better control the patch membrane potential. Experiments were conducted at room temperature (20-23°C).

For cell-attached recordings, pipette solution[12] contained (in mmol/L): KCl 5, NaCl 110, $MgCl_2$ 1, $CaCl_2$ 2, Hepes 10, pH=7.4 adjusted with NaOH. In some experiments, 0.1 µmol/L IBTX was added in the pipette solution. Generation of voltage commands and current acquisition were performed with Clampex (PClamp 10, Molecular Devices Inc.) through a Digidata 1440A and an Axopatch 200B amplifier (Axon CNS, Molecular Devices Inc., Sunnyvale, CA, USA). A gigaseal was obtained and current was recorded at patch potential (PP) of 40 mV (where PP= - applied voltage, due to the inverted output polarity in this configuration). Current was digitized at 10 kHz, filtered at 5 kHz (low pass Bessel filter). Different combinations of PDE inhibitors diluted in the bath solution were directly perfused over the cell using multiple pipes fused to a single manifold outlet. Perfusion with PDE inhibitor was started after the vehicle (DMSO 0.03%) had been perfused for 2-5 min and channel activity was stable. Ro and Cil superfusion immediately followed vehicle superfusion in 4 out of 11 cell-attached patches. In 4 other patches, (Ro+Cil) followed Ro alone superfusion, and the remaining 3 tests were following Cil alone superfusion.

For analysis, traces were further low-pass filtered offline at 2 kHz. Channel activity in patches was idealized using the single channel detection tool of Clampfit (PClamp 10, Molecular Devices Inc.). Cursors were positioned so that analysis ranged over a minimum of 45 s to 5 min period of stable channel activity (period of interest). Because a patch of cell membrane can often contain several active channels of undetermined number (N), indication of channel activity during a period of interest was given by the calculation of NP_o, the average number of

open channels (or the probability of any channel being open at any level), defined as follows[12, 13]:

$$NP_o = \sum_{L=0}^{N} L\, P_L$$

where P_L is the probability that L channels are open. P_L is given by the fraction of time spent by the current to a level corresponding to L channels opened, relative to the total duration of the period of interest. Mean open time was defined as the mean duration of a channel opening and given by[13]:

$$mean\ open\ time = NP_o/X$$

with X being the total number of opening transitions per unit of time. The opening frequency of N channels in the patch (NF_o) was given by dividing X by the total duration of the period of interest. Mean current amplitude (corresponding to the average amplitude of opening transitions at any level) were determined by a gaussian fit of amplitude histograms (bin width=0.2 pA). In case less than 10 events were present, arithmetic mean was used.

For inside-out recordings, the following pipette solution was used (in mmol/L): KCl 140, $MgCl_2$ 1, $CaCl_2$ 0.1, Hepes 10, pH=7.4 adjusted with KOH, allowing to work in symmetrical K^+ condition. Several PP were tested, each during 15-30 s, to build up the current-PP relationship of the conductance detected.

1.7 Western Blot analysis

Frozen LADCA were homogenized in ice-cold “Rippa” buffer containing 50 mmol/L Tris-HCl (pH=8), 150 mmol/L NaCl, 1% Triton X-100, 0.5% sodium deoxycholate, 0.1% SDS and a cocktail of protease and phosphatase inhibitors (cOmplete™ Protease Inhibitor CocktailTM, Sigma-Aldrich). Tissues were homogenized with a Precellys®24 (Bertin instrument, Montigny-Le-Bretonneux, France) for 10 s and kept in ice for few minutes. Supernatant was collected following centrifugation at 12000 *g*, 4°C for 5 min. Before electrophoresis, samples were prepared in fresh mix of Laemmli buffer and β-mercaptoethanol. Samples were generally heated at 95°C during 5 min except for BK_{Ca} detection where samples were kept on ice. Similar amounts of protein samples (50 µg) extracted from sham and HF rat LADCA were subjected to SDS-PAGE (8%) and electrotransferred onto PVDF membranes (Millipore, Molsheim, France). Membranes were then blocked with 5% non-fat dry milk dissolved in Tris-buffered saline containing 0.1% Tween-20 (TTBS) for 1 h for PDE detection or 2 h for BK_{Ca} α-subunit detection. Membranes were then incubated overnight at 4°C with primary antibodies: a rabbit polyclonal antibody anti-PDE3A (1/10000; kind gift from Dr. Chen Yan, University of Rochester

Medical Center, NY, USA), anti-PDE4A (1/5000), a rabbit polyclonal anti-PDE4B (1/1000), and anti-PDE4D (1/1000), kind gifts from Dr. Marco Conti (University of California, San Francisco, CA, USA), a mouse monoclonal antibody anti-BK_{Ca} α-subunit (1/500; #75-022, purchased from University of California Davis/NIH NeuroMab Facility), and anti-GAPDH (1/4000; #2118, Cell Signalling Technology, Danvers, MA, USA). After washing 3 times with TTBS, the membranes were incubated 1 h at room temperature with either horse anti-mouse IgG-HRP (1/3000; #7076, Cell Signalling) or goat anti-rabbit IgG-HRP (1/10000; #sc-2004, Santa Cruz Biotechnology Inc., Dallas, TX, USA). Detection was performed with chemiluminescence reagent (Pierce ECL Western blotting substrate, Thermo Fisher Scientific, Waltham, MA, USA). For quantification, tiff images were analyzed with ImageJ 1.50b software. Signals were submitted to densitometric analysis and GAPDH was used for normalization. Results were expressed relatively to the mean expression level in sham group. Controls for antibodies were provided by the manufacturer or available in Abi-Gerges et al. [14] and in Figure S2.

1.8 Proximity ligation assay (PLA)

Freshly isolated LADCA SMCs from HF and sham rats were seeded on glass coverslips and fixed in 4% (wt/vol) paraformaldehyde (PFA) prepared in phosphate buffered saline (PBS) for 10 min at room temperature. Following 3 washes with PBS, cells were permeabilized with 0.1% Triton X-100 and 0.2% BSA for 10 min at room temperature. Then, coverslips were incubated in a quenching solution (50 mmol/L NH_4Cl prepared in PBS) aiming at minimizing autofluorescence and washed 5 min in PBS. PLA protocol was carried out according to the recommendation of manufacturer (Duolink® PLA, Sigma-Aldrich). Primary antibodies were used at the indicated dilutions: anti-BK_{Ca} α-subunit (1/300), anti-PDE3A (1/400), anti-PDE4B (1/100), or a pan-PDE4 (rabbit polyclonal, 1/100; #PD4-101AP, FabGennix, Frisco, TX, USA). Preparations were incubated with anti-BK_{Ca} α-subunit antibody and one type of anti-PDE antibody (100 µL) overnight at 4°C. Preparations incubated with only one antibody were used as negative control. After washing, incubation of relevant secondary antibodies, ligation, and amplification were performed. After the final wash with appropriated buffer, the slides were washed with purified water and mounted in “Mowiol” medium (Mowiol® 4.88 g, glycerol 6 g, TrisHCl 0.2 mol/L; all compounds from Sigma-Aldrich) on glass slides. PLA images were acquired with a laser scanning confocal microscope (SP5, Leica Microsystems SAS, Nanterre, France) equipped with an x60 water immersion objective. The presence of PLA probes was revealed by excitation with a white light laser at 554 nm and emission was collected at 579 nm, using similar parameters for all slides testing a given antibody association. Because preliminary experiments using PDE4B and BK_{Ca} α-subunit antibodies led to saturating PLA signal (high fluorescence level and coalescence of the puncta), polymerization time for this

specific condition was reduced to 90 min (rather than 100 min) to dampen the signal. Tiff images were created and analyzed using the ImageJ 1.50b software. All single cell images corresponding to one given couple of antibodies were converted into 8-bit and binarized using a common threshold value. Threshold value was set arbitrarily to clearly discriminate fluorescence puncta from background. Results were expressed as the percentage of cell area covered by PLA signal. This technique allows to detect co-localization of proteins in a 40 nm range, based on the average diameter of an antibody being 10 nm (https://www.sigmaaldrich.com).

1.9 Histological evaluation coronary arteries

Following sacrifice some hearts were cannulated, perfused first 3 min with high K^+ Krebs and then with 10% formalin for 30 min at a flow rate of 8 mL/min. Hearts paraffin sections (5-µm thick) were stained by the trichrome method. Slides were scanned by the digital slide scanner NanoZoomer 2.0-RS (Hamamatsu, Palaiseau, France) allowing an overall view of the samples. Images were digitally captured from the scanned slides using the NDP.view2 software (Hamamatsu). Image analysis was performed using ImageJ software. Only arteries that were cut in cross section were analyzed. Because some remodeled arteries displayed expanded perivascular area, exact dimension of the vessel could not be determined accurately. Thus wall thickness (w) was defined as the thickness of media plus intima. It was measured as the mean distance between the limit of the lumen and the external limit of the media (identified as purple with distinct SMC, as opposed to bright blue area without cells that included fibrosis extending into the adventitia and myocardium). Between 6 and 14 values of wall thickness were taken for each vessel, depending on the regularity of the dimension. Luminal diameter (l) was defined as:

$$l = 2.\sqrt{L/\pi},$$

with L defined as the measured luminal area. Diameter of the vessel (d, excluding adventitia) was defined as:

$$d = l + 2w.$$

Only large arteries similar to the ones that were obtained after dissection were analysed. Diameters “d” of analyzed arteries averaged to 177±16 µm for sham (n= 23) and 188±16µm for HF (n=22). Data were expressed as: w/d in order to obtain an index of the thickness of the vascular wall proportionally to vessel size[15].

1.10 Data and statistical analysis

CRCs obtained for each vessel were fitted with the Hill equation using Prism 7 software (Graphpad Software, La Jolla, CA, USA) and pharmacological parameters, namely pD_2 and maximal effect (E_{max}), were obtained. pD_2 was defined as the negative logarithm of EC_{50}, giving the concentration of drug required to promote half maximal response. Data were expressed as mean ± SEM. N represented the number of rats while n represented the number of cells in electrophysiology and PLA experiments. Where relevant (values normally distributed), 2-group comparisons were performed using either t-test (variances equal) of or Welsh's t-test (variances unequal). When normality of distribution could not be assumed, non-parametric Mann-Whitney test was used. Paired comparisons were performed using the Wilcoxon signed-rank paired test to analyze the effect of addition of PDE inhibitors on the single channel activity *vs.* Control in the same cell. In comparisons involving more than 2 treatments, 1-way ANOVA followed by Holm-Sidak multiple comparison post-test was used. When comparing the effect of IBTX in sham and HF animals, 2-way ANOVA was used. Comparison of CRCs was performed using 2-way ANOVA for repeated measures. Values of $P<0.05$ were considered for statistical significance. Where relevant a nested ANOVA was performed to fit a mixed effects model. Comparison between sham and HF groups was treated as a fixed effect, while the animal was treated as a random effect. Nested ANOVA was performed using R software (R version 3.3.3, The R Foundation for Statistical Computing, www.r-project.org)[16].

2. Supplementary Tables

2.1 Table S1: Reference supporting selectivity of pharmacological inhibitors used.

Compound	**Concentration** (µmol/L)	**Target inhibited**	**Reference**
iberiotoxin (IBTX)	0.1	BK_{Ca} channel	Galvez et al., 1990 [5]
ryanodine	30	ryanodine receptor	Jaggar et al., 2000 [17], Sutko et al., 1997 [18]
DPO-1	1	K_v1 channel	Lagrutta et al. 2006 [19]
stromatoxin-1	0.1	K_v2 channel	Escoubas et al., 2002 [20]
XE991	30	K_v7 channel	Tsvetkov et al., 2017 [21]
glibenclamide	10	K_{ATP} channel	Standen et al., 1989 [22]
Ro-20-1724	10	PDE4	Rich et al., 2001 [9]
cilostamide	1	PDE3	Sudo et al., 2000 [8]

2.2 Table S2: Contraction level obtained in vascular reactivity experiments.

Abbreviations: ΔK80: amplitude of contractile response to K80 solution; ΔU46619: amplitude of contractile response to ΔU46619; endo.$^{(+)}$, endo.$^{(-)}$: with functional or non-functional endothelium, respectively; veh.^{water} veh.$^{DMSO\ 0.3\%}$, veh.$^{DMSO\ 0.01\%}$: vehicle incorporating 0.01%water, 0.3% DMSO or 0.01% DMSO, respectively; IBTX: iberiotoxin; glib: glibenclamide; DPO-1: Diphenyl phosphine oxide-1; STX: stromatoxin.

Table S2A: Contraction level obtained in experimental groups presented in **Figure 1.**

	endo.$^{(+)}$									endo.$^{(-)}$	
	veh.^{water}	IBTX 0.1 µmol/L	veh.$^{DMSO\ 0.3\%}$	ryanodine 30 µmol/L	veh.$^{DMSO\ 0.01\%}$	glib. 10 µmol/L	DPO-1 1 µmol/L	STX 0.1 µmol/L	XE991 30 µmol/L	veh.^{water}	IBTX 0.1 µmol/L
N	21	20	7	5	6	6	5	5	5	13	10
ΔK80 (mN/mm)	1.82 ± 0.11	1.94 ± 0.12	1.17 ± 0.14 $^{£}$	1.61 ± 0.32	1.85 ± 0.11	1.91 ± 0.16	1.58 ± 0.16	1.62 ± 0.24	1.68 ± 0.20	0.90 ± 0.07 $^{£££}$	0.92 ± 0.16
ΔU46619 (vs ΔK80)	1.12 ± 0.02	1.28 ± 0.04 **	1.15 ± 0.05	1.45 ± 0.10 $^{\#\#}$	1.14 ± 0.03	0.85 ± 0.08 §§	1.28 ± 0.06	1.10 ± 0.05	1.10 ± 0.04	1.11 ± 0.05	1.36 ± 0.05 ***

Statistics: data represent mean ± sem of N rats. **: P ≤ 0.01 vs relevant veh.^{water}; $^{\#\#}$: P ≤ 0.01 vs veh.$^{DMSO\ 0.3\%}$; §§: P ≤ 0.01 vs veh.$^{DMSO\ 0.01\%}$; $^{£}$: P ≤ 0.05, $^{£££}$: P ≤ 0.001 vs endo.$^{(+)}$ / veh.^{water} (ANOVA followed by Holm-Sidak's multiple comparison test).

Table S2B: Contraction level obtained in experimental groups presented in **Figure 3A-D (CRC isoprenaline)**

	veh.^{water}			IBTX		
	veh.^{DMSO}	Ro	Cil	veh.^{DMSO}	Ro	Cil
N	14	6	9	9	6	6
ΔK80 (mN/mm)	1.65 ± 0.09	1.98 ± 0.27	1.46 ± 0.18	1.95 ± 0.25	1.38 ± 0.11	1.79 ± 0.42
ΔU46619 (vs ΔK80)	1.01 ± 0.03	0.90 ± 0.04	1.00 ± 0.04	1.06 ± 0.02	0.98 ± 0.04	1.07 ± 0.06

Statistics: data represent mean ± sem of N rats. In this data set neither Ro, Cil nor IBTX had any significant effect compared to relevant vehicle (2-way ANOVA followed by Holm-Sidak's multiple comparison test).

Table S2C: Contraction level obtained in experimental groups presented in **Figure 3E-F (CRC L85)**.

	veh.^{water}			IBTX		
	veh.^{DMSO}	Ro	Cil	veh.^{DMSO}	Ro	Cil
N	13	8	9	6	7	9
ΔK80 (mN/mm)	1.48 ± 0.19	1.68 ± 0.21	1.57 ± 0.19	1.24 ± 0.17	1.65 ± 0.16	1.48 ± 0.16
ΔU46619 (vs ΔK80) $^{\#}$	1.04 ± 0.07	0.85 ± 0.07	1.05 ± 0.07	1.18 ± 0.08	1.20 ± 0.04	1.25 ± 0.04

Statistics: data represent mean ± sem of N rats. $^{\#}$: P ≤ 0.001, 2-way ANOVA (effect of factor "IBTX" vs "veh.^{water}"). Neither Ro nor Cil had any significant effect compared to relevant vehicle (2-way ANOVA followed by Holm-Sidak's multiple comparison test).

Table S2D: Contraction level obtained in experimental groups presented in **Figure 4**.

	sham		HF	
	veh.^{water}	IBTX	veh.^{water}	IBTX
N	7	6	7	6
ΔK80 (mN/mm) $^{\#}$	2.42 ± 0.23	2.30 ± 0.36	0.53 ± 0.11	0.47 ± 0.08
ΔU46619 (vs ΔK80)	1.00 ± 0.03	1.23 ± 0.03 *	1.21 ± 0.07	1.26 ± 0.11

Statistics: *: P ≤ 0.05 vs sham-veh.^{water} (2-way ANOVA followed by Holm-Sidak's multiple comparison test); $^{\#}$: P ≤ 0.001, 2-way ANOVA (effect of factor "HF" vs "sham").

2.3 Table S3: Effect of application of PDE inhibitors (Ro, 10 µmol/L, Cil, 1 µmol/L and Ro +Cil) on current amplitude, compared to DMSO. DMSO concentration was 0.03%, corresponding to the maximal DMSO concentration carried when Ro and Cil were added together. n: number of cell membrane patches studied from 5-7 animals. No significant effect on any parameter (Wilcoxon signed-rank test on patches or means per animals).

	n = 6	
	DMSO	Ro
current amplitude (pA)	4.05 ± 0.80	4.31 ± 0.71
	n = 6	
	DMSO	Cil
current amplitude (pA)	5.85 ± 1.31	5.74 ± 1.23
	n = 12	
	DMSO	Ro + Cil
current amplitude (pA)	5.82 ± 0.79	5.90 ± 0.55

2.4 Table S4: Echocardiographic and anatomic parameters in series of rats studied 22 weeks after aortic stenosis, or of sham-operated animals.

Abbreviations: IVSd and IVSs: end-diastolic and end-systolic interventricular septum thickness, respectively; LVPWd and LVPWs: end-diastolic and end-systolic LV posterior wall thickness; LVIDd and LVIDs: end-diastolic and end-systolic LV internal diameters, respectively; EDV and ESV: end-diastolic and end-systolic volume; FS: LV fractional shortening; EF: LV ejection fraction; SV: stroke volume; HR: heart rate (bpm: beat per minute); W/TL: weight of the indicated organ over tibia length ratio.

Echocardiographic parameters	**sham** (N = 11)	**aortic stenosis** (N = 14)	**P**
IVSd (mm)	1.42 ± 0.06	1.78 ± 0.08	**
IVSs (mm)	2.47 ± 0.15	2.72 ± 0.17	NS
LVPWd (mm)	1.78 ± 0.12	2.39 ± 0.16	**
LVPWs (mm)	2.83 ± 0.10	3,39 ± 0.18	*
LV mass (mg)	874 ± 48	1540 ± 156	***
LVIDd (mm)	7.69 ± 0.24	8.54 ± 0.27	*
LVIDs (mm)	4.12 ± 0.22	5.24 ± 0.33	*
FS (%)	46.6 ± 1.9	39.6 ± 2.3	*
EDV (mL)	1.03 ± 0.09	1.38 ± 0.12	*
ESV(mL)	0.19 ± 0.03	0.39 ± 0.06	**
SV(mL)	0.84 ± 0.07	1.00 ± 0.07	NS
EF(%)	82.3 ± 1.6	73.8 ± 2.7	*
HR (bpm)	334 ± 12	316 ± 8	NS
Anatomical parameters	**sham** (N = 11)	**aortic stenosis** (N = 11)	**P**
heart W/TL (mg/cm)	398 ± 16	690 ± 74	**
lung W/TL (mg/cm)	447 ± 17	641 ± 87	NS
liver W/TL (mg/cm)	3821 ± 155	4042 ± 207	NS
kidney W/TL (mg/cm)	355 ± 9	339 ± 18	NS
rat weight (g)	593 ± 17	603 ± 11	NS

Statistics: *: P<0.05, **: P<0.01, ***: P<0.001, NS: non-significant (t-test, Welsh's t-test or Mann and Whitney test when relevant, sham vs aortic stenosis surgery).

3. Supplemental References

1. De Sousa E, Veksler V, Minajeva A, Kaasik A, Mateo P, Mayoux E, Hoerter J, Bigard X, Serrurier B, Ventura-Clapier R. Subcellular creatine kinase alterations. Implications in heart failure. *Circ Res* 1999;**85**:68-76.
2. Feldman AM, Weinberg EO, Ray PE, Lorell BH. Selective changes in cardiac gene expression during compensated hypertrophy and the transition to cardiac decompensation in rats with chronic aortic banding. *Circ Res* 1993;**73**:184-192.
3. Prunier F, Gaertner R, Louedec L, Michel JB, Mercadier JJ, Escoubet B. Doppler echocardiographic estimation of left ventricular end-diastolic pressure after mi in rats. *Am J Physiol Heart Circ Physiol* 2002;**283**:H346-352.
4. Teichholz LE, Kreulen T, Herman MV, Gorlin R. Problems in echocardiographic volume determinations: Echocardiographic-angiographic correlations in the presence or absence of asynergy. *Am J Cardiol* 1976;**37**:7-11.
5. Galvez A, Gimenez-Gallego G, Reuben JP, Roy-Contancin L, Feigenbaum P, Kaczorowski GJ, Garcia ML. Purification and characterization of a unique, potent, peptidyl probe for the high conductance calcium-activated potassium channel from venom of the scorpion buthus tamulus. *J Biol Chem* 1990;**265**:11083-11090.
6. Gautier M, Hyvelin JM, de Crescenzo V, Eder V, Bonnet P. Heterogeneous K_v1 function and expression in coronary myocytes from right and left ventricles in rats. *Am J Physiol Heart Circ Physiol* 2007;**292**:H475-482.
7. Thompson WJ, Appleman MM. Multiple cyclic nucleotide phosphodiesterase activities from rat brain. *Biochemistry* 1971;**10**:311-316.
8. Sudo T, Tachibana K, Toga K, Tochizawa S, Inoue Y, Kimura Y, Hidaka H. Potent effects of novel anti-platelet aggregatory cilostamide analogues on recombinant cyclic nucleotide phosphodiesterase isozyme activity. *Biochem Pharmacol* 2000;**59**:347-356.
9. Rich TC, Tse TE, Rohan JG, Schaack J, Karpen JW. In vivo assessment of local phosphodiesterase activity using tailored cyclic nucleotide-gated channels as camp sensors. *J Gen Physiol* 2001;**118**:63-78.
10. Nyborg NC, Baandrup U, Mikkelsen EO, Mulvany MJ. Active, passive and myogenic characteristics of isolated rat intramural coronary resistance arteries. *Pflugers Arch* 1987;**410**:664-670.
11. Hamill OP, Marty A, Neher E, Sakmann B, Sigworth FJ. Improved patch-clamp techniques for high-resolution current recording from cells and cell-free membrane patches. *Pflugers Arch* 1981;**391**:85-100.
12. White RE, Darkow DJ, Lang JL. Estrogen relaxes coronary arteries by opening BK_{Ca} channels through a cgmp-dependent mechanism. *Circ Res* 1995;**77**:936-942.
13. Singer JJ, Walsh JVJ. Characterization of calcium-activated potassium channels in single smooth muscle cells using the patch-clamp technique. *Pflugers Arch* 1987;**408**:98-111.
14. Abi-Gerges A, Richter W, Lefebvre F, Mateo P, Varin A, Heymes C, Samuel JL, Lugnier C, Conti M, Fischmeister R, Vandecasteele G. Decreased expression and activity of cAMP phosphodiesterases in cardiac hypertrophy and its impact on β-adrenergic camp signals. *Circ Res* 2009;**105**:784-792.
15. Schwartzkopff B, Motz W, Frenzel H, Vogt M, Knauer S, Strauer BE. Structural and functional alterations of the intramyocardial coronary arterioles in patients with arterial hypertension. *Circulation* 1993;**88**:993-1003.
16. Mangiafico SS. *An r companion for the handbook of biological statistics*. version 1.3.2., 2015.

17. Jaggar JH, Porter VA, Lederer WJ, Nelson MT. Calcium sparks in smooth muscle. *Am J Physiol Cell Physiol* 2000;**278**:C235-256.
18. Sutko JL, Airey JA, Welch W, Ruest L. The pharmacology of ryanodine and related compounds. *Pharmacol Rev* 1997;**49**:53-98.
19. Lagrutta A, Wang J, Fermini B, Salata JJ. Novel, potent inhibitors of human $K_v1.5$ K^+ channels and ultrarapidly activating delayed rectifier potassium current. *J Pharmacol Exp Ther* 2006;**317**:1054-1063.
20. Escoubas P, Diochot S, Celerier ML, Nakajima T, Lazdunski M. Novel tarantula toxins for subtypes of voltage-dependent potassium channels in the K_v2 and K_v4 subfamilies. *Mol Pharmacol* 2002;**62**:48-57.
21. Tsvetkov D, Kassmann M, Tano JY, Chen L, Schleifenbaum J, Voelkl J, Lang F, Huang Y, Gollasch M. Do $K_v7.1$ channels contribute to control of arterial vascular tone? *Br J Pharmacol* 2017;**174**:150-162.
22. Standen NB, Quayle JM, Davies NW, Brayden JE, Huang Y, Nelson MT. Hyperpolarizing vasodilators activate ATP-sensitive K^+ channels in arterial smooth muscle. *Science* 1989;**245**:177-180.

Supplementary Figures

(contains Figures S1 to S3)

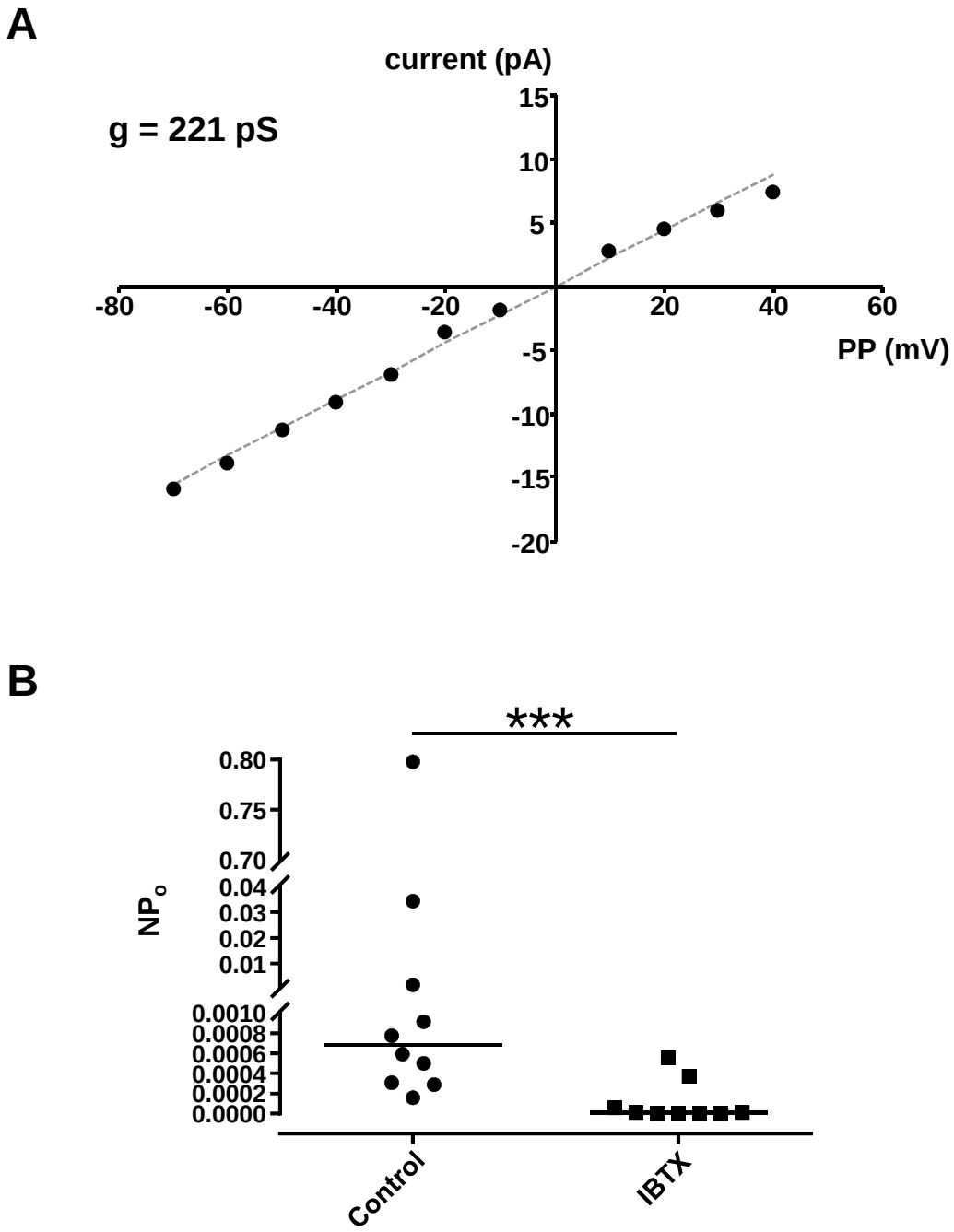

Figure S1. Characterization of BK_{Ca} single channel activity in rat LDCA SMCs. A. Using inside-out patches in symmetrical $[K^+]$ and high Ca^{2+} ($[K^+]$=140 mmol/L, $[Ca^{2+}]$=0.1 mmol/L), a unitary conductance (g) of 221 pS was measured (average of 2 patches). **B.** Using cell-attached patches under physiological $[K^+]$ gradient ($[K^+]$ in pipette=5 mmol/L), specific BK_{Ca} inhibitor IBTX (0.1 µmol/L) nearly abolished NP_o (*i.e.* the average number of open channels) when present in the pipette solution. Patch potential=40 mV. n=9-10 cells from N=3 rats. **: P<0.01 (Mann and Whitney test).

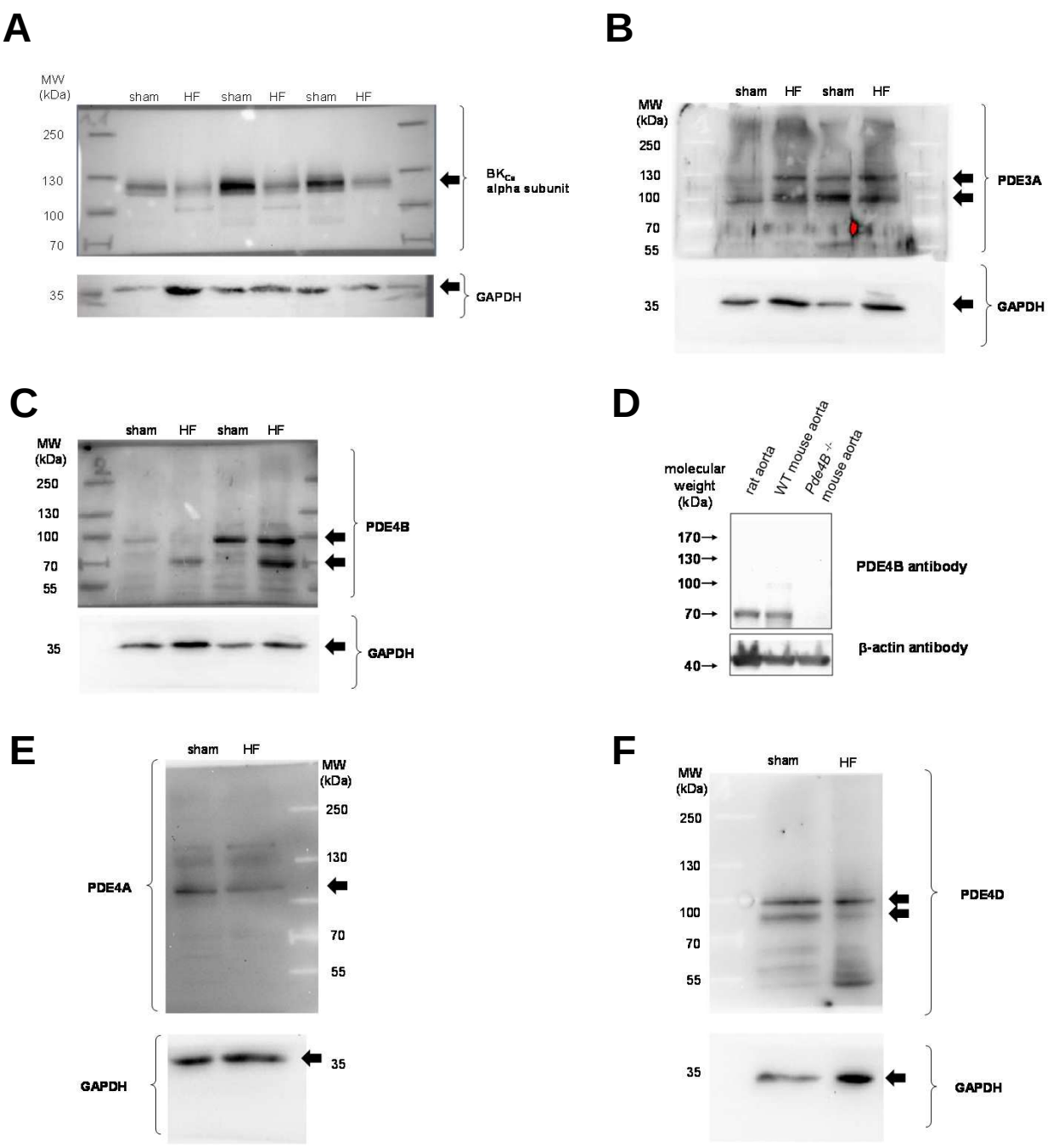

Figure S2. Examples of full length blots for BK_{Ca} alpha subunit (**A**), PDE3A (**B**), PDE4B (**C**), PDE4A (**E**) and PDE4D (**F**) using sham and HF rat LADCA samples. **D**: western blot showing the signal detected by the anti-PDE4B antibody in aorta from rat, a *Pde4B*$^{-/-}$ mouse and a wild type littermate. MW: molecular weight marker (kDa).

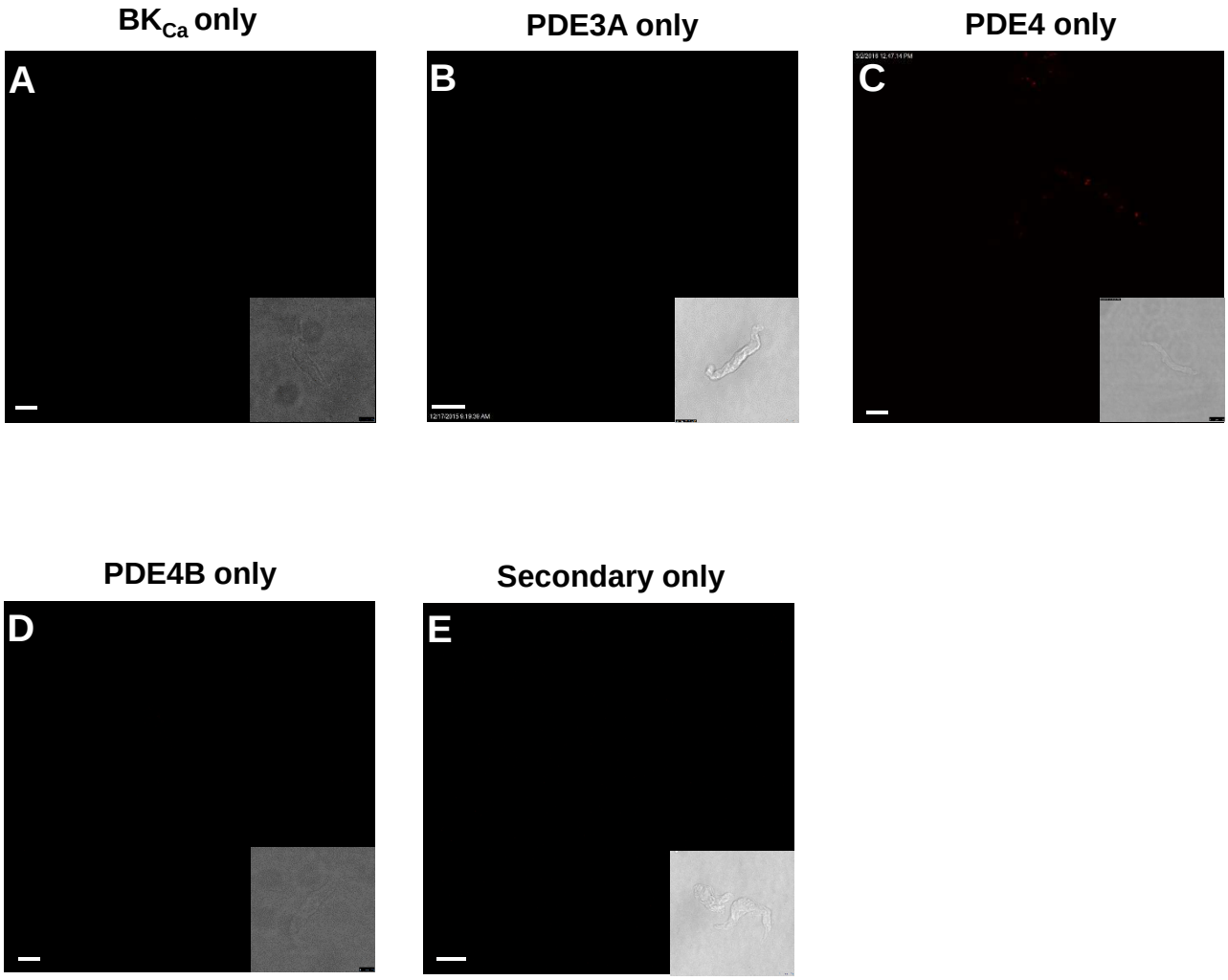

Figure S3. Negative control experiments of *in situ* PLA using the following primary antibodies: anti-BK_{Ca} α-subunit alone (**A**), anti-PDE3A alone (**B**), anti-PDE4 alone (**C**), an anti-PDE4B alone (**D**), or relevant pair of Duolink® oligonucleotide-associated secondary antibodies (**E**), in rat LDCA SMCs. **A**, **B**, **C**, **D** and **E** are representative confocal images. Scale bar: 5 µm. Inset shows transmitted light images.